

BEAM THEORY FOR STRONGLY ORTHOTROPIC MATERIALS

MARCO SAVOIA and NERIO TULLINI

University of Bologna, Faculty of Engineering, Istituto di Tecnica delle Costruzioni,
Viale Risorgimento 2, 40136, Bologna, Italy

(Received 29 July 1994; in revised form 17 July 1995)

Abstract—This paper presents a displacement-based model for orthotropic beams under plane linear elasticity based on the only kinematic assumption of transverse inextensibility. Any given axial and transverse loading as well as boundary conditions at the beam ends are considered. The solution is decomposed into the principal and the residual part (corresponding to the interior and the boundary problems) which are obtained by series expansions of polynomial functions and eigenfunctions, respectively. It is proved that the proposed one-dimensional theory gives both interior and boundary exact two-dimensional elasticity solutions for strongly orthotropic materials, i.e. for ratio between shear modulus and axial Young modulus approaching zero. For isotropic and orthotropic materials the accuracy of the beam model is also analysed and compared with that of other theories. In particular, the complementary energy error of the interior solution with respect to two-dimensional elasticity is evaluated, the asymptotic estimate of the characteristic decay length of end effects given in Choi and Horgan [*J. Appl. Mech. ASME*, **44**, 424-430 (1977)] by two-dimensional analysis is reobtained and the range of validity of boundary solution is discussed. The numerical results presented agree very well with exact and finite element solutions even in the neighbourhood of clamped cross-sections, where the solution is mainly governed by the boundary problem. Copyright © 1996 Elsevier Science Ltd.

1. INTRODUCTION

The increasing use of advanced composites for structural applications has represented the main motivation to develop refined theories for single-layer or multi-layered orthotropic beams and plates where the limits of classical theories are removed [see for instance Kapania and Raciti (1989) and Reddy and Robbins (1994)]. In fact, due to the strongly directional nature of materials properties of fibre composites, 'non-classical' effects such as transverse shear deformation, cross-sectional axial warping and slow stress decay from end sections are much more pronounced than for isotropic materials.

It is well known that the classical Saint-Venant warping is exact only for beams with unrestrained ends and tip loads. For more complex conditions, as local loading and short wavelength vibrational modes, higher order warpings and end effects become very important (Tsai and Soler, 1970; Savoia *et al.*, 1993a). For these reasons, the range of validity of linear and non-linear beam theories (Levinson, 1981; Rehfield and Murthy, 1982; Atligan *et al.*, 1991; Ie and Kosmatka, 1992; Renton, 1991; Cesnik and Hodges, 1993) that consider Saint-Venant in-plane and out-of-plane warpings only for the computation of cross-sectional stiffness constants (tension modulus, bending modulus, etc.) should be assessed carefully. For instance, stress concentrations due to warping restrained cannot be predicted.

As far as two-dimensional plane elasticity approaches are concerned, most of the solutions proposed in the literature refer to interior problems only, i.e. without taking the pointwise boundary conditions at the beam extremities into account. In particular, for transversely loaded isotropic beams Donnell (1952), Boley and Tolins (1956), Gatewood and Dale (1962) and Soler (1968) used polynomial expansion of stress components. Stress fields for orthotropic beams subject to uniform and linearly varying transverse loads can also be found in Rehfield and Murthy (1982) and Rychter (1988). The presence of local loading has been considered in Tsai and Soler (1970) and Renton (1991), where classical theory is shown to severely underestimate maximum stresses. It is worth noting that, when the interior problem only is considered, no other details can be prescribed at the beam ends

but shear stress resultants, bending moments, average vertical deflections and section rotations.

Duva and Simmonds (1990) developed a formal asymptotic expansion technique to generate approximate strain and stress fields of "any accuracy" for orthotropic (possibly weak in shear) beams. Their technique is very interesting, since it can be used in several cases to obtain *exact* two-dimensional interior solutions, satisfying both equilibrium and bi-harmonic compatibility equations. The same authors gave asymptotic expressions (for height-to-length ratio approaching zero) of corrections to lateral deflection and natural frequencies predicted by the elementary theory when effects due to built-in ends are considered (Duva and Simmonds, 1991). Asymptotic analysis of orthotropic semi-infinite elastic strips subject to end loads or displacements have been performed by Horgan and Simmonds (1991). For the ratio between shear modulus and axial Young modulus approaching zero, the boundary solution in terms of Airy stress function has been obtained as a *wide* boundary layer, decaying slowly in the axial direction, plus a *narrow* boundary layer, decaying over a shorter distance when compared with the beam height.

The idea of splitting the equations of theory of elasticity into a one-dimensional problem (theory of rods) and a two-dimensional problem (the section problem) allowed the study of non-linear static and dynamic problems, including the elastic coupling phenomena between extensional and shear deformations for anisotropic beams (Berdichevsky, 1981; Cesnik and Hodges, 1993). In this framework, the approaches proposed in Giavotto *et al.* (1983), Bauchau (1985) and Borri and Merlini (1986) (devoted to linear and non-linear analysis of spatial behaviour of anisotropic beams) should be mentioned, where an eigenfunction superposition technique is used to obtain the solution for the beam end zones. In these papers, only loads applied at the end sections are considered, and the eigenfunctions are obtained by a two-dimensional finite element analysis.

Several displacement-based one-dimensional models for homogeneous and laminated beams have been proposed, where the transverse displacement is assumed to be constant over the height and the axial displacement is represented by means of a linear combination of assigned coordinate functions and unknown functions defined along the beam axis [see, for instance, Bickford (1982), Bauchau (1985), Hjelmstad (1987), Reddy (1987), Heyliger and Reddy (1988), Savoia *et al.*, (1993a)]. In this case, variational or equilibrium methods are used to obtain the set of differential equations for the unknown functions, by facing interior and boundary problems simultaneously. Even though these models account for any kind of transverse load, as well as a wide class of end conditions (including clamped or stress-free end sections), pointwise equilibrium equations and stress-free conditions at the lateral surfaces are usually not satisfied.

In the present paper, a displacement-based one-dimensional beam theory is developed making use of the only assumption of inextensibility in the transverse direction. In the spirit of constrained elasticity (Truesdell and Noll, 1965; Podio Guidugli, 1989), the introduction of an internal constraint in the space of admissible deformations results in the decomposition of the stress tensor into an active and a reactive part; since the reactive part (which contains the only transverse normal stress for the problem at hand) is defined by the condition of null work for any admissible deformation, the virtual work principle is used to derive a set of integral-differential equations involving the active part of the stress tensor only. The problem is then formulated by decomposing the solution into a principal and a residual part, corresponding to the interior and the boundary problems, respectively.

With reference to a beam subject to a general transverse and axial loading condition, the interior problem is solved by means of a series expansion in terms of a complete system of polynomial functions. This set of polynomials provides for a closed form solution if transverse and axial loads vary along the beam according to a polynomial law. Displacement and stress components for the interior problem are given as functions of axial load resultant, distributed moment, shear resultant and their derivatives. It is shown that average shear strain depends on even derivatives of shear resultant through a set of shear correction factors which are explicitly given. The complementary energy error of the proposed one-dimensional theory with respect to two-dimensional elasticity is computed analytically. It is shown that, unlike classical models, the error of the proposed solution tends to zero for

strongly orthotropic materials, i.e. for ratio between shear modulus and axial Young modulus approaching zero.

The boundary problem is solved by the Fourier' method making use of a complete set of orthogonal eigenfunctions, defined so as to satisfy pointwise equilibrium equations and boundary conditions at the lateral faces in the axial direction. The completeness of eigenfunctions is established in the context of theory of integral operators. Also in this case, it is proved that the proposed boundary solution gives the exact two-dimensional elasticity solution for strongly orthotropic materials. In particular, the *wide* boundary layer obtained in Horgan and Simmonds (1991) and the asymptotic estimates of the characteristic decay length of end effects given in Choi and Horgan (1977) for both stretching and flexure problems are recovered. The range of validity of the boundary solution is discussed through comparison with eigenvalues and eigenvectors given by two-dimensional elasticity.

Numerical comparisons with exact and finite element solutions show that the proposed beam theory yields very accurate results even in the neighbourhood of clamped cross-sections, where the solution is governed by the boundary problem. For isotropic and orthotropic cantilever beams under flexure at infinity the results obtained are in good agreement with Gregory and Gladwell's (1982) and Lin and Wan's (1990) two-dimensional solutions, including the stress singularity arising at the corner points of the clamped cross-section. It is also shown that boundary effects which arise when the interior solution does not satisfy stress-free end conditions are less pronounced than those due to the presence of clamped cross-sections. Hence, for simply-supported beams under uniformly distributed transverse load, axial normal stresses at the mid-span given by the only interior solution are shown to be accurate also for moderately thick beams ($\ell/H > 4$).

2. GOVERNING EQUATIONS

A beam with rectangular cross-section is referred to a Cartesian reference frame $0x_1x_2$, where x_1, x_2 axes are chosen in the axial and the transverse direction, respectively (Fig. 1). The thickness is considered sufficiently narrow so that plane stress hypothesis applies. The beam is made of homogeneous, orthotropic, linearly elastic material, with the orthotropy axes coinciding with the reference axes. The beam occupies the region $\Omega = [0, \ell] \times [-h, h]$, where $H = 2h$ and ℓ are the total height and length, and is subject to tractions $\mathbf{q}_t \equiv (q_{1t}, q_{2t})$ and $\mathbf{q}_b \equiv (q_{1b}, q_{2b})$ at the top and the bottom faces, either tractions $\mathbf{f} \equiv (f_1, f_2)$ or displacements $\bar{\mathbf{u}} \equiv (\bar{u}_1, \bar{u}_2)$ at the end sections and no body force (Fig. 1). We further assume that there are no discontinuities in $\mathbf{q}, \mathbf{f}, \bar{\mathbf{u}}$ distributions and their derivatives.

Several methods have been proposed for the solution of this elasticity problem, where displacement components or the Airy stress function are represented in terms of series expansion by a complete set of functions, e.g. power functions, Legendre's polynomials or

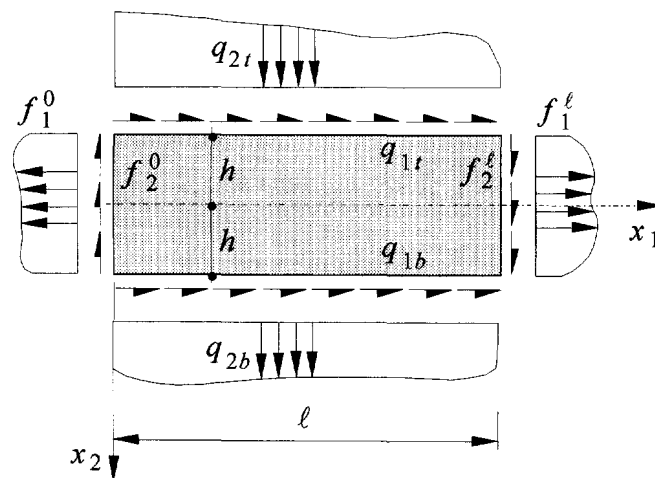


Fig. 1. Orthotropic rectangular beam and notation for displacements and loads.

eigenfunctions (Donnell, 1952; Hashin, 1967; Soler, 1968; Timoshenko and Goodier, 1970; Choi and Horgan, 1977; Mathúna, 1989).

Nevertheless, when the height is sufficiently small with respect to the length, or the Young modulus in the x_1 direction is significantly larger than that in the transverse direction, approximations for transverse displacement are often introduced [see, for instance, Antman and Warner (1966), Sayir (1980), Massonet (1983)]. In this context, one-dimensional beam models usually neglect both transverse deformation and transverse stress component σ_{22} . These two conditions can be simultaneously satisfied by deriving the one-dimensional constitutive law in the context of constrained elasticity, requiring that the active part only of the stress tensor be involved (Truesdell and Noll, 1965). Then, constraint equation and constitutive relations reduce to:

$$u_{2,2} = 0 \quad (1)$$

$$\sigma_{11} = E_1 u_{1,1}, \quad \sigma_{12} = G_{12}(u_{1,2} + u_{2,1}) \quad (2)$$

where E_1 is the Young modulus in the x_1 direction, G_{12} is the shear modulus and comma denotes partial differentiation. Assumption (1) is very common in the derivation of two-dimensional classical and higher-order theories for homogeneous/laminated plates and shells [see, for instance, Naghdi (1972), Librescu (1975), Lewinski (1987), Reddy (1987), Savoia *et al.* (1994)]. For two-dimensional bodies the constitutive equations replacing eqns (2) are given in terms of the well-known reduced elastic coefficients. Relations which allow the recovery of three-dimensional (two-dimensional) displacement, strain and stress fields starting from the results of two-dimensional (one-dimensional) analyses have been obtained in Atligan and Hodges (1992) and Savoia (1995) for laminated plates (beams). It has been shown (Savoia, 1995) that eqns (1) and (2) satisfy the Koiter (1970) consistency condition, i.e. statically-admissible and kinematically-admissible stress fields can be derived from eqns (2), whose relative energy error approaches zero with the height-to-length ratio. By integrating eqn (1), the transverse displacement u_2 constant over the beam height is obtained:

$$u_2(x_1, x_2) = v(x_1). \quad (3)$$

In the spirit of Kantorovich's method, eqn (3) is equivalent to retaining the first term only in a transverse displacement expansion.

The only reactive stress component due to the presence of the internal constraint of transverse inextensibility (1) is the normal stress σ_{22} . An energy-consistent displacement-based model can be obtained by direct substitution of the assumed displacement field into the two-dimensional virtual work equation (Lewinski, 1987). In fact, the virtual work principle provides for the direct derivation of the set of equilibrium equations involving the active stress components only (Truesdell and Noll, 1965). Making use of eqns (3), this variational equation states:

$$\int_{\Omega} [\sigma_{11} \tilde{u}_{1,1} + \sigma_{12} (\tilde{u}_{1,2} + \tilde{u}_{2,1})] d\Omega - \int_0^l [q_{1b} \tilde{u}_1|_{x_2=-h} + q_{1t} \tilde{u}_1|_{x_2=h} + (q_{2b} + q_{2t}) \tilde{u}_2] dx_1 - \left[\int_{-h}^h (f_1 \tilde{u}_1 + f_2 \tilde{u}_2) dx_2 \right]_0^l = 0 \quad (4)$$

to hold for every kinematically admissible displacement field $\tilde{u}_1(x_1, x_2)$, $\tilde{u}_2(x_1, x_2) = \tilde{v}(x_1)$. In eqn (4) the work done by any transverse load distributions $q_{2b}(x_1)$, $q_{2t}(x_1)$ applied at the top and bottom faces depends on the section resultant $q_2 = q_{2b} + q_{2t}$ only. Making use of the standard procedure of variational calculus, eqn (4) yields the following set of equilibrium equations:

$$\sigma_{11,1} + \sigma_{12,2} = 0, \quad \frac{dQ}{dx_1} = -q_2 \quad \text{in } \Omega \quad (5)$$

$$\sigma_{12}(x_1, h) = q_{1b}, \quad \sigma_{12}(x_1, -h) = -q_{1t} \quad \text{at } x_2 = h, -h \quad (6)$$

$$\sigma_{11} = f_1, \quad \text{or } u_1 = \bar{u}_1 \quad \text{at } x_1 = 0, \ell \quad (7a)$$

$$Q = \bar{F}_2 \quad \text{or } v = \bar{v} \quad \text{at } x_1 = 0, \ell \quad (7b)$$

where:

$$Q(x_1) = \int_{-h}^h \sigma_{12} dx_2, \quad \bar{F}_2 = \int_{-h}^h f_2 dx_2 \quad (8)$$

are the inner shear resultant and the resultant of the transverse load $f_2(x_2)$ applied at the end sections, respectively. Overbars denote prescribed values at the beam end sections. Due to the assumption of transverse inextensibility, equilibrium equations in the transverse direction can only be imposed in a global form, see eqns (5b) and (7b).

The solution to eqns (2), (3) and (5)–(7) can be obtained by decomposing each of the unknown functions into a couple of additive terms, i.e. the principal and the residual part of the solution, corresponding to the interior and the boundary problem, respectively (Donnell, 1976; Ladevèze, 1983).

As for the interior problem, stress and displacement distributions, prescribed at the end sections according to eqns (7a), are replaced by their average values:

$$\{N, M\} = \{\bar{F}_1, \bar{M}\} \quad \text{or } \{u_a, \varphi\} = \{\bar{u}_a, \bar{\varphi}\} \quad \text{at } x_1 = 0, \ell \quad (9)$$

where, for a unit thickness,

$$\{N, M\} = \int_{-h}^h \sigma_{11} \{1, x_2\} dx_2, \quad \{\bar{F}_1, \bar{M}\} = \int_{-h}^h f_1 \{1, x_2\} dx_2 \quad (10)$$

collect the axial force and the bending moment at the inner and end cross-sections, respectively. Moreover,

$$\{u_a, \varphi\} = \int_{-h}^h u_1 \left\{ \frac{1}{2h}, -\frac{3}{2h^3} x_2 \right\} dx_2 \quad (11)$$

represent the average axial displacement and rotation of the cross-section.

In conclusion, the principal part of the solution is required to satisfy field equations (5) and pointwise stress balance at the lateral faces (6), together with average boundary conditions (9) at the beam ends.

The residual part of the solution, which is required to re-establish the pointwise boundary conditions (7a), is characterised by null external loads q_{1b} , q_{1t} , q_2 , null axial, bending and shear resultants N , M , Q along the beam as well as null average axial displacement and rotation u_a , φ . Hence, the governing equations for the boundary problem reduce to:

$$\sigma_{11,1} + \sigma_{12,2} = 0, \quad Q = 0 \quad \text{on } \Omega \quad (12)$$

$$\sigma_{12}(x_1, h) = 0, \quad \sigma_{12}(x_1, -h) = 0 \quad (13)$$

$$\sigma_{11}^r = f_1 - \sigma_{11}^p \quad \text{or } u_1^r = \bar{u}_1 - u_1^p \quad \text{at } x_1 = 0, \ell \quad (14)$$

where superscripts p and r in eqns (14) refer to the principal and residual part of the

solution, respectively. Saint-Venant's principle assures that the non-vanishing stress fields given by the boundary problem are restricted to portions in the vicinity of end sections, whose length depends on the degree of orthotropy of the material (Choi and Horgan, 1977). Moreover, the assumption of transverse inextensibility (1) restricts the class of boundary phenomena which can be described: eqns (14) show that end effects arising from pointwise distributions of applied shear forces $f_2(x_2)$ or transverse displacement $\bar{u}_2(x_2)$ cannot be considered.

Introducing the dimensionless variables:

$$x = \frac{x_1}{\ell}, \quad y = \frac{x_2}{h} \quad (15)$$

the beam domain reduces to $[0, 1] \times [-1, 1]$.

In Sections 3 and 4, both the interior and the boundary problem are solved by expanding the axial displacement u_1 in terms of a linear combination of a complete system of functions $U_n(y)$ and unknown functions $\Phi_n(x)$. Then, the displacement field is written as:

$$\begin{aligned} u_1(x, y) &= h \sum_{n=0}^{\infty} \Phi_n(x) U_n(y) \\ u_2(x) &= \ell \eta(x) \end{aligned} \quad (16)$$

where $\eta(x) = v(x)/\ell$ is the non-dimensional transverse displacement. Moreover, substituting eqns (16) in eqns (2), the following expressions for normal and shear stresses are obtained:

$$\begin{aligned} \sigma_{11}(x, y) &= E_1 \frac{h}{\ell} \sum_{n=0}^{\infty} \Phi'_n(x) U_n(y) \\ \sigma_{12}(x, y) &= G_{12} \left(\eta'(x) + \sum_{n=0}^{\infty} \Phi_n(x) \frac{dU_n(y)}{dy} \right) \end{aligned} \quad (17)$$

where prime denotes the total derivative with respect to x . Finally, the reactive stress component σ_{22} can be determined by integrating the pointwise two-dimensional equilibrium equation in the transverse direction:

$$\sigma_{22}(x, y) = -q_{2t} - \frac{h}{\ell} \int_{-1}^y \sigma_{12,x} \, d\hat{y} \quad (18)$$

3. THE INTERIOR PROBLEM

3.1. Formulation

As far as the interior problem is concerned, the functions $U_n(y)$ in eqn (16) are chosen as polynomials $P_n(y)$ defined according to the following recursive formulas:

$$P_0 = 1, \quad P_1 = y, \quad \text{and} \quad \frac{d^2 P_n}{dy^2} = -\rho P_{n-2} \quad \text{for } n \geq 2 \quad (19)$$

where the dimensionless parameter ρ is defined as:

$$\rho = \frac{E_1 h^2}{G_{12} \ell^2} \tag{20}$$

Equation (19c) is integrated by means of the following conditions :

$$\int_{-1}^1 P_n dy = \int_{-1}^1 P_n y dy = 0 \quad \text{for } n \geq 2. \tag{21}$$

Making use of the Müntz' theorem (Courant and Hilbert, 1953, p. 102), it is easy to verify that eqns (19) define a complete set of polynomials. As will be shown in the following, this set of coordinate functions is particularly appropriate since it provides for the closed form solution by means of a finite number of terms in eqn (16a), for external loads varying along x according to a polynomial law. Moreover, the conditions (21) identify the functions $h\Phi_0$ and $-\Phi_1$ with the average axial displacement u_0 and the average cross-sectional rotation φ defined in eqn (11), as can be verified by substituting eqn (16a) in eqn (11).

By imposing the conditions (21), the following (recursive) solution of the differential equation (19c) is obtained :

$$P_2(y) = \rho \frac{1-3y^2}{6}, \quad P_{2n+2}(y) = \rho \left[-\frac{1}{2} \int_0^1 t(2-t)P_{2n}(t) dt - \int_0^y (y-t)P_{2n}(t) dt \right]$$

for $n \geq 1$

$$P_3(y) = \rho \frac{3y-5y^3}{30}, \quad P_{2n+3}(y) = \rho \left[\frac{y}{2} \int_0^1 (2+t^3)P_{2n+1}(t) dt - \int_0^y (y-t)P_{2n+1}(t) dt \right]$$

for $n \geq 1$. (22)

The polynomials P_{2n}, P_{2n+1} given by eqn (22) are even and odd functions of y , respectively. By direct computation, the derivatives of polynomials P_2, P_3 at the top and bottom faces become :

$$\frac{dP_2(\pm 1)}{dy} = \mp \rho, \quad \frac{dP_3(\pm 1)}{dy} = -\frac{2}{5}\rho, \tag{23}$$

Substituting eqn (19c) in eqns (21) and performing an integration by parts, the following values are obtained for the higher order polynomials :

$$\frac{dP_n(\pm 1)}{dy} = \frac{1}{2}[P_n(1) - P_n(-1)] \quad \text{for } n \geq 4 \tag{24a}$$

or, equivalently,

$$\frac{dP_{2n}(\pm 1)}{dy} = 0 \quad \frac{dP_{2n+1}(\pm 1)}{dy} = P_{2n+1}(1) \quad \text{for } n \geq 2 \tag{24b}$$

for the even and odd polynomials, respectively.

Substituting eqn (17b) in the stress balance conditions reported in eqns (6), and taking eqns (20, 23) into account, straightforward algebra yields the following expressions for the lateral deflection η and function Φ_2 :

$$\eta'(x) = \frac{m(x)}{G_{12}A} - \sum_{n=0}^{\infty} \Phi_{2n+1}(x) \frac{dP_{2n+1}(1)}{dy} \quad (25)$$

$$\Phi_2(x) = -\frac{1}{h} \frac{q_1(x)\ell^2}{E_1A} \quad (26)$$

where $A = H \cdot 1 = 2h$ is the cross-sectional area and

$$q_1(x) = q_{1b}(x) + q_{1t}(x), \quad m(x) = [q_{1b}(x) - q_{1t}(x)]h \quad (27)$$

are the resultant and the moment resultant of axial load distributions at the top and bottom faces. Eqn (25) shows that the polynomials of even order P_{2n} give no contribution to the lateral deflection. Further, substituting eqn (17b) in equilibrium equation (5b), identifying functions U_n with polynomials P_n and performing the integration along the beam axis yield:

$$G_{12}A \left(\eta'(x) + \sum_{n=0}^{\infty} \Phi_{2n+1}(x) P_{2n+1}(1) \right) = Q(x) \quad (28)$$

where the shear resultant $Q(x)$ is defined as:

$$Q(x) = \bar{F}'_2 + \ell \int_x^1 q_2(t) dt. \quad (29)$$

Making use of eqns (20), (24b) and (25), eqn (28) reduces to:

$$\Phi_3(x) = \frac{T(x)\ell^2}{E_1I} \quad (30)$$

where $I = 2h^3/3$ is the second area moment and

$$T(x) = Q(x) - m(x). \quad (31)$$

Finally, substituting axial and shear stresses (17) in equilibrium equation (5a) yields:

$$\rho \sum_{n=0}^{\infty} \Phi_n''(x) P_n(y) + \sum_{n=2}^{\infty} \Phi_n(x) \frac{d^2 P_n(y)}{dy^2} = 0 \quad (32)$$

which, employing recursive formulas (19c) for the polynomials P_n , reduces to:

$$\rho \sum_{n=0}^{\infty} (\Phi_n''(x) - \Phi_{n+2}(x)) P_n(y) = 0. \quad (33)$$

Taking the linear independence of the polynomials P_n into account and making use of eqns (26) and (30) for Φ_2 and Φ_3 , the following expressions for the remaining unknown functions Φ_n are obtained:

$$\Phi_0''(x) = -\frac{1}{h} \frac{q_1\ell^2}{E_1A}, \quad \Phi_{2n}(x) = -\frac{1}{h} \frac{q_1^{(2n-2)}\ell^2}{E_1A} \quad (34)$$

$$\Phi_1''(x) = \frac{T\ell^2}{E_1I}, \quad \Phi_{2n+1}(x) = \frac{T^{(2n-2)}\ell^2}{E_1I} \quad (35)$$

where $(\cdot)^{(n)}$ denotes the n th derivative with respect to the axial coordinate x and eqns (26) and (30) represent a particular case of eqns (34) and (35) when $n = 1$.

Equations (34) and (35) show that the interior problem can be separated into two uncoupled problems, related to the symmetric and the antisymmetric part of the applied loads with respect to the beam axis. The symmetric part defines the stretching problem, the antisymmetric part governs the flexure problem. Furthermore, eqns (34a) and (35a) coincide with the basic equations of classical Euler–Bernoulli theory and must be integrated making use of boundary conditions (9), which are written in terms of unknown functions Φ_0 and Φ_1 as follows:

$$\{\Phi'_0, \Phi'_1\} = \left\{ \frac{\ell}{h} \frac{\bar{F}_1}{E_1 A}, \frac{\bar{M}\ell}{E_1 I} \right\} \quad \text{or} \quad \{h\Phi_0, \Phi_1\} = \{\bar{u}_a, -\bar{\varphi}\} \quad \text{at } x = 0, 1. \quad (36)$$

The set of polynomials (22) adopted is particularly appropriate for the solution of the interior problem. In fact, the unknown functions Φ_n can be explicitly obtained for any given axial and transverse loading. On the contrary, when power or Legendre polynomial expansions over the beam height are used, a coupled system of differential equations is obtained, whose solution can be very burdensome (Soler, 1968; Tsai and Soler, 1970; Mathùna, 1989).

In the following, stretching and flexure solutions will be studied separately.

3.2. *Stretching problem*

Equations (16)–(18), (25) and (34) yield the following displacement and stress fields for the stretching problem (Fig. 2a), valid for any given loading condition:

$$\begin{aligned} u_1 &= \Phi_0 h - \frac{\ell^2}{E_1 A} \sum_{n=1}^{\infty} q_1^{(2n-2)} P_{2n}, & \sigma_{11} &= E_1 \frac{h}{\ell} \Phi'_0 - \frac{\ell}{A} \sum_{n=1}^{\infty} q_1^{(2n-1)} P_{2n} \\ \sigma_{12} &= -\frac{1}{2\rho} \sum_{n=1}^{\infty} q_1^{(2n-2)} \frac{dP_{2n}}{dy}, & \sigma_{22} &= \frac{h}{2\rho\ell} \sum_{n=1}^{\infty} q_1^{(2n-1)} [P_{2n}(y) - P_{2n}(1)]. \end{aligned} \quad (37)$$

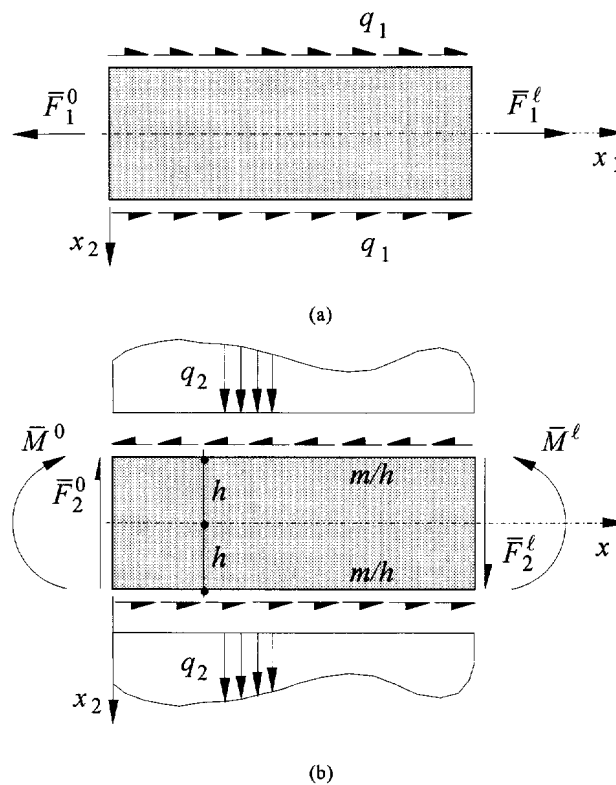


Fig. 2. (a) Stretching problem. (b) Bending problem.

Equation (37a) states that the axial displacement $u_1(x, y)$ depends on the axial load resultant q_1 defined in eqn (27a) as well as on all its even derivatives. Moreover, it is given by a finite number of terms $N = \text{int}[p/2] + 1$ if the axial load varies along the beam according to a polynomial law of order p . Making use of eqn (22), eqns (37) can be made explicit as:

$$\begin{aligned}
 u_1 &= \Phi_0 h - \frac{\rho \ell^2}{E_1 A} \left[\frac{q_1}{6} (1 - 3y^2) + \frac{\rho q_1''}{360} (7 - 30y^2 + 15y^4) \right. \\
 &\quad \left. + \frac{\rho^2 q_1^{(4)}}{15120} (31 - 147y^2 + 105y^4 - 21y^6) + \dots \right] \\
 \sigma_{11} &= \frac{N}{A} - \frac{\rho \ell}{A} \left[\frac{q_1'}{6} (1 - 3y^2) + \frac{\rho q_1^{(3)}}{360} (7 - 30y^2 + 15y^4) + \dots \right] \\
 \sigma_{12} &= \frac{1}{A} \frac{h}{\ell} y \left[q_1 \ell + \frac{\rho q_1' \ell}{6} (1 - y^2) + \frac{\rho^2 q_1^{(4)} \ell}{360} (7 - 10y^2 + 3y^4) + \dots \right] \\
 \sigma_{22} &= \frac{1}{A} \frac{h^2}{\ell^2} (1 - y^2) \left[\frac{q_1' \ell}{2} + \frac{\rho q_1^{(3)} \ell}{24} (1 - y^2) + \frac{\rho^2 q_1^{(5)} \ell}{720} (1 - y^2) (3 - y) + \dots \right] \quad (38)
 \end{aligned}$$

where the axial resultant $N(x)$, given by:

$$N(x) = \bar{F}'_1 + \ell \int_x^1 q_1(t) dt \quad (39)$$

has been introduced by integrating eqn (34a) once and substituting it and eqn (37b) in eqn (10a).

3.3. Flexure problem

As for the flexure problem (Fig. 2b), eqns (25) and (35) show that the average shear strain $\eta' + \Phi_1$ is a function of the distributed moment $m(x)$, of $T(x)$ defined in eqn (31) as well as of its even derivatives:

$$\eta' + \Phi_1 = \frac{m}{G_{12} A} - \frac{\ell^2}{E_1 I} \sum_{n=1}^{\infty} T^{(2n-2)} \frac{dP_{2n+1}(1)}{dy} \quad (40)$$

Making use of eqns (20) and (24b), eqn (40) can be rewritten as:

$$\eta' + \Phi_1 = \frac{m}{G_{12} A} + \sum_{n=0}^{\infty} \frac{T^{(2n)}}{k_n G_{12} A} \quad (41)$$

where:

$$\frac{1}{k_0} = \frac{6}{5}, \quad \frac{1}{k_1} = \frac{\rho}{175}, \quad \frac{1}{k_2} = \frac{2\rho^2}{7875}, \dots, \quad \frac{1}{k_n} = -\frac{3}{\rho} P_{2n+3}(1) \quad \text{for } n \geq 1 \quad (42)$$

represent the shear correction factors corresponding to $T(x)$ and its even derivatives. The first correction factor k_0 coincides with that obtained by Cowper (1966) and Renton (1991) for constant shear resultant and Poisson' ratio equal to zero. The subsequent correction factors k_1, k_2, \dots , multiplying the even derivatives of $T(x)$, are required for non-uniform transverse loads. Equivalent definitions of shear correction factors have been obtained in Savoia *et al.* (1993a) for multi-layered beams, by adopting a set of piecewise orthogonal polynomials which reduce to Legendre polynomials for homogeneous beams. The dependence of shear correction factor on the loading condition was already pointed out by

Berdichevsky and Krashnina (1976) in the derivation of the second-order approximation of their asymptotically exact beam theory. Equation (41) shows that, for a given arbitrary load, it is not possible to define a unique shear correction factor k_0 ; this can be done only for simple loadings, such as shear resultant varying according to a trigonometric law, $T(x) = \cos(m\pi x)$, where eqn (41) yields the following relation for the average shear strain:

$$\eta' + \Phi_1 = \frac{T(x)}{\bar{k}G_{12}A}, \quad \text{where } \frac{1}{\bar{k}} = \frac{6}{5} - \frac{3}{\rho} \sum_{n=1}^{\infty} (-1)^n (m\pi)^{2n} P_{2n+3}(1) \quad (43)$$

is the shear factor, which still depends on the rapidity of variation of the load along the beam. It is shown in Appendix A that a sufficient condition for the convergence of the series appearing in eqn (43b) holds for $\rho < 2.05/m^2$, that is for $\ell/h > 1.35m\sqrt{E_1/G_{12}}$.

Finally, making use of eqns (16)–(18) and (35), the following expressions are obtained for the axial displacement and the stress components, valid for a beam subject to a general resultant $T(x) = Q(x) - m(x)$:

$$\begin{aligned} u_1 &= h \left(\Phi_1 y + \frac{\ell^2}{E_1 I} \sum_{n=1}^{\infty} T^{(2n-2)} P_{2n+1} \right) \\ \sigma_{11} &= E_1 \frac{h}{\ell} \Phi_1' y + \frac{h\ell}{I} \sum_{n=1}^{\infty} T^{(2n-1)} P_{2n+1} \\ \sigma_{12} &= \frac{1}{A} \left[m + \frac{3}{\rho} \sum_{n=1}^{\infty} T^{(2n-2)} \left(\frac{dP_{2n+1}(y)}{dy} - \frac{dP_{2n+1}(1)}{dy} \right) \right] \\ \sigma_{22} &= -q_{2t} - \frac{h}{Al} \left\{ m'(1+y) + \frac{T'}{2}(2+3y-y^3) + \frac{3}{\rho} \sum_{n=2}^{\infty} T^{(2n-1)} [P_{2n+1}(y) - yP_{2n+1}(1)] \right\}. \end{aligned} \quad (44)$$

Making use of eqn (22), eqns (44) can be made explicit as:

$$\begin{aligned} u_1 &= h \left\{ \Phi_1 y + \frac{\rho \ell^2}{E_1 I} \left[\frac{T}{30}(3y-5y^3) + \frac{\rho T''}{4200}(27y-70y^3+35y^5) \right. \right. \\ &\quad \left. \left. + \frac{\rho^2 T^{(4)}}{378000}(133y-405y^3+315y^5-75y^7) + \dots \right] \right\} \\ \sigma_{11} &= \frac{Mhy}{I} + \frac{1}{A} \frac{E_1 h}{G_{12} \ell} \left[\frac{T'}{10}(3y-5y^3) + \frac{\rho T^{(3)}}{1400}(27y-70y^3+35y^5) + \dots \right] \\ \sigma_{12} &= \frac{1}{A} \left[m + \frac{3T}{2}(1-y^2) + \frac{\rho T''}{40}(1-6y^2+5y^4) + \frac{\rho^2 T^{(4)}}{8400}(11-81y^2+105y^4-35y^6) + \dots \right] \\ \sigma_{22} &= -q_{2t} - \frac{1}{A} \frac{h}{\ell} \left[m'(1+y) + \frac{T'}{2}(2+3y-y^3) + \frac{\rho T^{(3)}}{40}(y-2y^3+y^5) + \dots \right] \end{aligned} \quad (45)$$

where the bending moment $M(x)$, defined as:

$$M(x) = \bar{M}' - \bar{F}'_2 \ell (1-x) + \ell \int_x^1 [(x-t)q_2(t)\ell + m(t)] dt \quad (46)$$

has been introduced by integrating eqn (35a) once and substituting it and eqn (44b) in eqn (10a).

In the normal stress given by eqn (45b), the first term on the right-hand side corresponds to the usual linear distribution of the classical theory, whereas each term reported in parenthesis gives a self-equilibrated stress distribution, related to the variation of cross-sectional warping along the beam. This phenomenon, called 'shear-lag' has already been pointed out in the analysis of beams with compact (Timoshenko and Goodier, 1970; Rehfield and Murthy, 1982; Massonet, 1983), thin-walled (Reissner, 1946; Laudiero and Savoia, 1990) and laminated (Savoia *et al.*, 1993a, 1993b) cross-section subject to uniformly distributed transverse loads. Equation (44b) shows that, for a transverse load varying according to a polynomial law of order p , a number $N = \text{int}[p/2 + 1]$ of self-equilibrated normal stress distributions can be introduced corresponding to as many warping modes.

4. THE BOUNDARY PROBLEM

The solution of the boundary problem defined in eqns (12)–(14) is obtained by means of Fourier method. To this purpose, by substituting eqns (17) in the field equation (12a), the following eigenvalue problem is obtained:

$$\frac{d^2 U_n}{dy^2} + \lambda_n^2 U_n = 0, \quad \Phi_n'' - \gamma_n^2 \Phi_n = 0 \quad (47)$$

where λ_n is the eigenvalue and

$$\gamma_n = \frac{\lambda_n}{\sqrt{\rho}} = \lambda_n \frac{\ell}{h} \sqrt{\frac{G_{12}}{E_1}} \quad (48)$$

is the dimensionless decay rate. By solving eqn (47a), two sets of orthogonal eigenfunctions, even and odd functions of y , respectively, are obtained:

$$U_n^e(y) = \cos \lambda_n^e y, \quad U_n^o(y) = \sin \lambda_n^o y / \sin \lambda_n^o. \quad (49)$$

Substituting eqns (17b) and (8a) in the null shear resultant condition (12b), the lateral deflection corresponding to the even and the odd part of the boundary solution are obtained:

$$\eta_c' = 0, \quad \eta_o' = - \sum_{n=1}^{\infty} \Phi_n(x). \quad (50)$$

Hence, making use of eqns (49) and (50), the boundary conditions (13) reduce to:

$$\frac{dU_n^e(\pm 1)}{dy} = 0, \quad \frac{dU_n^o(\pm 1)}{dy} = U_n^o(1) \quad (51)$$

and give the following characteristic equations for even and odd eigenvalues:

$$\lambda_n^e = n\pi \quad (52)$$

$$\tan \lambda_n^o = \lambda_n^o. \quad (53)$$

The completeness of eigenfunctions (49) is well established, since eqn (47a) represents a standard Sturm–Liouville eigenvalue problem [Courant and Hilbert (1953) p. 360 and Appendix A]. Analogously, the proof of the completeness of the eigenfunctions associated with the stresses [see eqns (17) and (18)] can be found in Horgan and Simmonds (1991).

In order to impose the boundary conditions (14) at the beam ends, the polynomials P_n in eqn (22) are expanded in terms of eigenfunctions as follows (see Appendix A) :

$$P_{2n} = -2\rho^n \sum_{j=1}^{\infty} \frac{(-1)^j}{\lambda_j^{e^{2n}}} \cos \lambda_j^e y, \quad P_{2n+1} = -\frac{2\rho^n}{3} \sum_{j=1}^{\infty} \frac{1}{\lambda_j^{o^{2n}}} \frac{\sin \lambda_j^o y}{\sin \lambda_j^o} \quad \text{for } n \geq 1. \quad (54)$$

Equations (54) clearly show that the even and odd polynomials P_{2n} and P_{2n+1} used for the interior problem, are proportional, as $n \rightarrow \infty$, to the first even and odd eigenfunction [$n = 1$ in eqns (49)].

The solution to the differential equation (47b) can be cast in the form :

$$\Phi_n(x) = A_n \cosh \gamma_n x + B_n \sinh \gamma_n x. \quad (55)$$

Integration constants A_n, B_n are determined by imposing boundary conditions (14) which, making use of Fourier method, are rewritten in the form of uncoupled equations for the unknown functions $\Phi_n(x)$ as :

$$\Phi_n = \bar{u}_n - u_n \quad \text{or} \quad \Phi'_n = \bar{s}_n - s_n \quad \text{at } x = 0, 1 \quad (56)$$

where :

$$\{\bar{u}_n, u_n\} = \frac{1}{h} \int_{-1}^1 \{\bar{u}_1, u_1^p\} U_n dy, \quad \{\bar{s}_n, s_n\} = \frac{\ell}{E_1 h} \int_{-1}^1 \{f_1, \sigma_{11}^p\} U_n dy \quad (57)$$

and superscript p denotes the principal part of the solution obtained in the previous section. Making use of eqns (37a,b), (44a,b) and (54), the Fourier coefficients u_n and s_n of the principal part of the solution can be written in terms of derivatives of the axial load and shear resultant as :

$$\begin{aligned} \{u_n, s_n\} &= (-1)^n \frac{2}{G_{12} A} \frac{h}{\ell} \sum_{j=0}^{\infty} \frac{\rho^j}{\lambda_n^{e^{2j+2}}} \{q_1^{(2j)} \ell, q_1^{(2j+1)} \ell\} \\ & \quad \text{at } x = 0, 1 \quad (58) \\ \{u_n, s_n\} &= -\frac{2}{G_{12} A} \sum_{j=0}^{\infty} \frac{\rho^j}{\lambda_n^{o^{2j+2}}} \{T^{(2j)}, T^{(2j+1)}\} \end{aligned}$$

for stretching and flexure problem, respectively. Of course, if polynomial loads are considered, the principal part of the solution and, consequently, the summations in eqns (58) reduce to a finite number of terms.

As an example, for a cantilever beam under general loading and perfectly clamped at $x = 0$, i.e. $\bar{u}_1(0, y) = 0$, the boundary conditions (56) for the n th unknown functions yield $\Phi_n(0) = -u_n^0, \Phi'_n(1) = \bar{s}_n^{\ell} - s_n^{\ell}$, and eqn (55) reduces to :

$$\Phi_n(x) = -u_n^0 \varphi_n(x) + (\bar{s}_n^{\ell} - s_n^{\ell}) \frac{\sinh \gamma_n x}{\gamma_n \cosh \gamma_n} \quad (59)$$

where :

$$\varphi_n(x) = \cosh \gamma_n x - \tanh \gamma_n \sinh \gamma_n x. \quad (60)$$

Analogously, for a simply-supported beam boundary conditions (56) reduce to $\Phi'_n(0) = \bar{s}_n^0 - s_n^0, \Phi'_n(1) = \bar{s}_n^{\ell} - s_n^{\ell}$ and eqn (55) gives :

$$\Phi_n(x) = \frac{1}{\gamma_n} \left[(\bar{s}_n^{\ell} - s_n^{\ell}) \frac{\cosh \gamma_n x}{\sinh \gamma_n} - (\bar{s}_n^0 - s_n^0) \frac{\varphi_n(x)}{\tanh \gamma_n} \right]. \quad (61)$$

5. COMPARISON BETWEEN ONE-DIMENSIONAL AND ELASTICITY SOLUTION

In this section the accuracy of the one-dimensional beam theory is assessed for both interior and boundary solutions through comparison with that given by theory of elasticity.

5.1. Accuracy of interior solution

The interior problem of a cantilever beam loaded by a transverse shear force \bar{F}'_2 at $x = \ell$ and clamped at $x = 0$ is considered first. By imposing the vanishing of average rotation at $x = 0$, average shear strain and axial displacement given by two-dimensional elasticity are:

$$\begin{aligned}\eta' + \Phi_1 &= \frac{6}{5} \frac{\bar{F}'_2}{G_{12}A} \left[1 + \frac{\nu_{12}G_{12}}{4E_1}(1-5y^2) \right] \\ u_1 &= h \left[\Phi_1 y + \rho \left(1 - \nu_{12} \frac{G_{12}}{E_1} \right) \frac{\bar{F}'_2 \ell^2}{30E_1 I} (3y - 5y^3) \right]\end{aligned}\quad (62)$$

where ν_{12} is the Poisson' ratio and $\Phi_1 = -\bar{F}'_2 \ell^2 x(2-x)/(2E_1 I)$.

First of all, it can be verified that the stress components given by eqns (45) coincide with those derived from the exact two-dimensional solution (62). Moreover, eqns (62) reduce to the solution given by eqns (41) and (44a) when strongly orthotropic beams are considered, i.e. if the term $\nu_{12}G_{12}/E_1$ becomes negligible.

As for the more general case of a transverse load varying according to a polynomial law, the asymptotic expansion technique proposed by Duva and Simmonds (1990) yields the exact two-dimensional stress field and can be used as the reference solution. For instance, according to their technique, for a transverse load $q_2(x)$ given by a parabolic law and split in two equal parts acting at the top and bottom faces ($q_{2b} = q_{2t} = q_2/2$), the following exact stress field can be derived:

$$\begin{aligned}\sigma_{11}^{2D} &= \frac{Mhy}{I} + \frac{1}{A} \frac{\bar{E}h}{\ell} \left\{ \frac{Q'}{10}(3y-5y^3) + \frac{\bar{\rho}Q^{(3)}}{1400} [27y-70y^3+35y^5-5\epsilon^2(39y-70y^3+7y^5)] \right\} \\ \sigma_{12}^{2D} &= \frac{1}{A} \left[\frac{3Q}{2}(1-y^2) + \frac{\bar{\rho}Q''}{40}(1-6y^2+5y^4) \right] \\ \sigma_{22}^{2D} &= -\frac{1}{A} \frac{h}{\ell} \left[\frac{Q'}{2}(3y-y^3) + \frac{\bar{\rho}Q^{(3)}}{40}(y-2y^3+y^5) \right]\end{aligned}\quad (63)$$

where $\bar{\rho} = \bar{E}h^2/\ell^2$, $\bar{E} = E_1/G_{12} - 2\nu_{12}$ and:

$$\epsilon = \frac{1}{\bar{E}} \sqrt{\frac{E_1}{E_2}} = \frac{G_{12}}{\sqrt{E_1 E_2}} \frac{1}{1 - 2\nu_{12} \frac{G_{12}}{E_1}}.\quad (64)$$

It is easy to verify that eqns (63) reduce to eqns (45b-d) by replacing \bar{E} with E_1/G_{12} and neglecting the terms containing the factor ϵ defined in eqn (64) (this circumstance holds also for higher-order loads). These two conditions typically hold for unidirectional strongly orthotropic materials, whose elastic coefficients are characterised by the following order of magnitudes:

$$E_1 = O(E), \quad G_{12} = O(1), \quad E_2 = O(1), \quad \nu_{12} = O(1) \quad \text{for } E \rightarrow \infty. \quad (65)$$

Hence, the stress field corresponding to two-dimensional theory of elasticity asymptotically reduces to that given by the proposed theory for strongly orthotropic materials.

A quantitative estimate of the accuracy of the one-dimensional interior solution can be performed by computing the mean-square error of the statically-admissible stress field (45) with respect to the exact solution (63). For a cantilever beam subject to a uniformly distributed transverse load ($q_{2b} = q_{2t} = q/2$), making use of the norm for the stress tensor based on the complementary elastic energy :

$$\|\boldsymbol{\sigma}\|^2 = h\ell \int_0^1 \int_{-1}^1 \left(\frac{\sigma_{11}^2}{E_1} + \frac{\sigma_{22}^2}{E_2} - 2\frac{v_{12}}{E_1} \sigma_{11}\sigma_{22} + \frac{\sigma_{12}^2}{G_{12}} \right) dx dy \quad (66)$$

the error of stress field (45) with respect to the exact solution (63) is:

$$e^{1D} = \frac{\|\boldsymbol{\sigma}^{1D} - \boldsymbol{\sigma}^{2D}\|}{\|\boldsymbol{\sigma}^{2D}\|} = \frac{2v_{12}/\bar{E}}{\left[1 + 85\varepsilon^2 + 2\frac{v_{12}}{\bar{E}} + \frac{280}{\bar{E}} \left(\frac{\ell}{H} \right)^2 \left(1 + 3\frac{v_{12}}{\bar{E}} \right) + \frac{420}{\bar{E}^2} \left(\frac{\ell}{H} \right)^4 \right]^{1/2}}. \quad (67)$$

It is easy to verify that for strongly orthotropic materials, having $\bar{E} \rightarrow \infty$ and $\varepsilon \rightarrow 0$, eqn (67) states that the energy error tends to zero.

As for the Euler–Bernoulli model, the corresponding error e^{EB} with respect to the exact solution is obtained in a form analogous to eqn (67), with $2v_{12}/\bar{E}$ at the numerator to be replaced by 1. Hence, for a given ℓ/H ratio, the energy error for Euler–Bernoulli model tends to a finite value (100%) when $\bar{E} \rightarrow \infty$. Moreover, the complementary energy errors for the proposed and the Euler–Bernoulli model admit the following asymptotic expressions for very thick ($\ell/H \rightarrow 0$) and slender ($\ell/H \rightarrow \infty$) beams :

$$\lim_{\ell/H \rightarrow 0} e^{1D} = \frac{2v_{12}/\bar{E}}{\left[1 + 85\varepsilon^2 + 2\frac{v_{12}}{\bar{E}} \right]^{1/2}}, \quad \lim_{\ell/H \rightarrow \infty} e^{1D} = \frac{v_{12}}{\sqrt{105}} \left(\frac{H}{\ell} \right)^2 \quad (68)$$

$$\lim_{\ell/H \rightarrow 0} e^{EB} = \frac{1}{\left[1 + 85\varepsilon^2 + 2\frac{v_{12}}{\bar{E}} \right]^{1/2}}, \quad \lim_{\ell/H \rightarrow \infty} e^{EB} = \frac{\bar{E}}{2\sqrt{105}} \left(\frac{H}{\ell} \right)^2. \quad (69)$$

In order to illustrate this result, the mean-square errors for uniformly loaded isotropic ($\nu = 0.3$) and orthotropic ($E_1/G_{12} = 50$, $E_1/E_2 = 25$, $\nu_{12} = 0.3$) cantilever beams is reported in Fig. 3 as a function of length-to-height ratio. The figure confirms the asymptotic predictions of eqns (68) and (69); it is worth noting that the Taylor expansion of eqn (67), which has been used to obtain eqns (68b) and (69b), holds for $\ell/H > 1.43$ and $\ell/H > 5.82$ for the isotropic and the orthotropic case, respectively.

5.2. Accuracy of boundary solution

It can be shown that the boundary problem given by the theory of elasticity reduces asymptotically to that given by the proposed theory for strongly orthotropic materials. To this purpose, consider the Airy stress function F , such that $\sigma_{11} = F_{,22}$, $\sigma_{12} = -F_{,12}$, $\sigma_{22} = F_{,11}$. Selecting a decaying solution of the form $F(x, y) = e^{-\gamma_{2D}x} \psi(y)$, where $\gamma_{2D} = \lambda_{2D}/\sqrt{\rho}$ and λ_{2D} is the eigenvalue with $\text{Re}(\lambda_{2D}) > 0$, the generalised biharmonic equation, giving the strain compatibility condition, yields (Choi and Horgan, 1977; Horgan and Simmonds, 1991) :

$$\frac{d^4\psi}{dy^4} + \lambda_{2D}^2 \frac{d^2\psi}{dy^2} + \varepsilon^2 \lambda_{2D}^4 \psi = 0. \quad (70)$$

Since $\varepsilon \rightarrow 0$ for strongly orthotropic materials, if λ_{2D} is bounded eqn (70) reduces to:

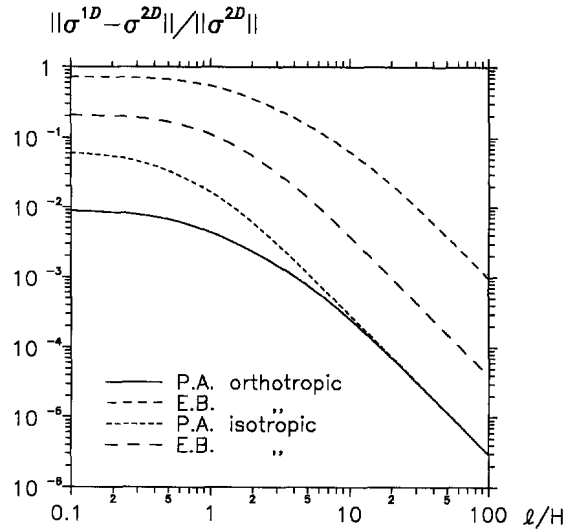


Fig. 3. Mean-square error of stress fields given by the present analysis and Euler–Bernoulli model for the interior solution of isotropic ($\nu = 0.3$) and orthotropic ($E_1/G_{12} = 50$, $E_1/E_2 = 25$, $\nu_{12} = 0.3$) cantilever beams under uniformly distributed load.

$$\frac{d^4\psi}{dy^4} + \bar{\lambda}^2 \frac{d^2\psi}{dy^2} = 0, \quad \text{where } \bar{\lambda} = \lambda_{2D}|_{\varepsilon=0}, \tag{71}$$

whose even and odd general integrals are given by :

$$\psi_n^e = a_n + b_n \cos \bar{\lambda}_n^e y, \quad \psi_n^o = c_n y + d_n \sin \bar{\lambda}_n^o y, \tag{72}$$

subject to :

$$\frac{d\psi(\pm 1)}{dy} = 0, \quad \psi(\pm 1) = 0 \tag{73}$$

corresponding to the stress-free boundary conditions $\sigma_{12} = \sigma_{22} = 0$ at the lateral faces. Substituting eqns (72) in eqns (73), the characteristic eqns (52) and (53) are identically reobtained, so that $\bar{\lambda}_n^e = \lambda_n^e$ and $\bar{\lambda}_n^o = \lambda_n^o$. As for the eigenfunctions, setting $U_n = d^2\psi_n/dy^2$ it is easy to verify that eqn (47a) reduces to eqn (71); correspondingly, the two-dimensional stress components σ_{11} , σ_{12} , σ_{22} reduce asymptotically to those given by one-dimensional theory.

For an orthotropic material with $E_1/G_{12} = 50$, $E_1/E_2 = 25$ and $\nu_{12} = 0.3$ (resulting in $\varepsilon = 0.101215$), Table 1 shows that the eigenvalues given by eqns (52) and (53) are in good agreement with the exact two-dimensional solution by Choi and Horgan (1977), the error being less than 3.5% for the first 10 even and odd modes. The percentage error refers to the real part of the eigenvalue, which is typically used to evaluate the exponential decay rate of the eigenfunction. It is worth noting that the percentage error of the set of eigenfunctions obtained here does not increase if higher-order modes are considered. Moreover, the first two even and odd modes for the normal stress σ_{11} given by eqns (49) are reported in Fig. 4, showing excellent agreement with the exact two-dimensional eigenfunctions.

In order to assess the range of validity of the one-dimensional boundary solution, Fig. 5 shows the first three even and odd eigenvalues λ_{2D} obtained from eqns (70) and (73)†. The numerical values reported in Fig. 5 correspond to eigenvalues with double multiplicity, which represent the transition between real and complex eigenvalues. The figures confirm the asymptotic behaviour ($\varepsilon \rightarrow 0$) of eigenvalues predicted by one-dimensional theory, and

† The first even eigenvalue reported in Fig. 5a is plotted in Crafter *et al.* (1993) and Wang *et al.* (1993) for the anisotropic elastic strip.

Table 1. Eigenvalues for a strongly orthotropic beam in plane stress : $E_1/G_{12} = 50$, $E_1/E_2 = 25$, $\nu_{12} = 0.3$, resulting in $\epsilon = 0.101215$ [see eqn (64)] : comparison between exact two-dimensional solution (Choi and Horgan, 1977) and present one-dimensional model. The percentage error refers to the real part of the eigenvalue

| Mode | Symmetric | | | Antisymmetric | | |
|------|-----------|------------------------------|-------|--------------------------|-------------------------------|-------|
| | $n\pi$ | Two-dimensional | Re(%) | $\tan \lambda = \lambda$ | Two-dimensional | Re(%) |
| 1 | 3.1415927 | 3.1925866 | -1.60 | 4.4934095 | 4.5329374 | -0.87 |
| 2 | 6.2831853 | 6.3940457 | -1.73 | 7.7252518 | 7.7940322 | -0.88 |
| 3 | 9.4247780 | 9.6258415 | -2.09 | 10.904122 | 11.003144 | -0.90 |
| 4 | 12.566371 | 13.020685 | -3.49 | 14.066194 | 14.197861 | -0.93 |
| 5 | 15.707963 | 15.545391 $\pm 1.188110i$ | 1.05 | 17.220755 | 17.389563 | -0.97 |
| 6 | 18.849556 | 18.653547 | 1.05 | 20.371303 | 20.586171 | -1.04 |
| 7 | 21.991149 | 21.975503 | 0.07 | 23.519453 | 23.801549 | -1.19 |
| 8 | 25.132741 | 25.196879 | -0.25 | 26.666054 | 27.091162 | -1.57 |
| 9 | 28.274334 | 28.395294 | -0.43 | 29.811599 | 30.628082 | -2.67 |
| 10 | 31.415927 | 31.587234 | -0.54 | 32.956389 | $\pm 1.0595979i$ 32.643108 | 0.96 |

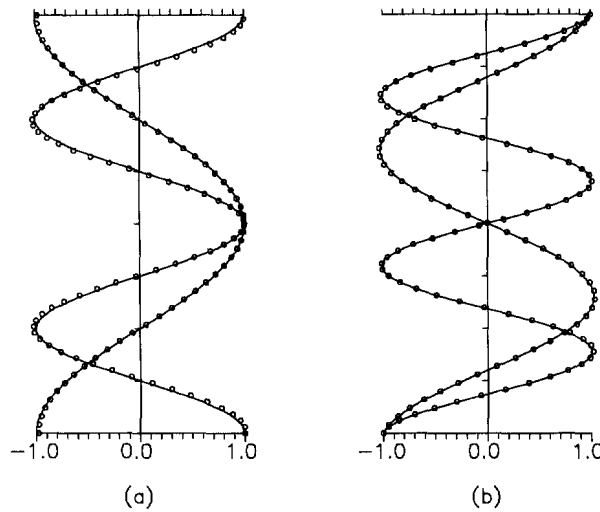


Fig. 4. The first two (a) even and (b) odd modes for the normal stress for a typical strongly orthotropic beam : $E_1/G_{12} = 50$, $E_1/E_2 = 25$, $\nu_{12} = 0.3$ ($\epsilon = 0.101215$) ; — : present one-dimensional model ; $\circ\circ\circ$: exact two-dimensional solution (Choi and Horgan, 1977).

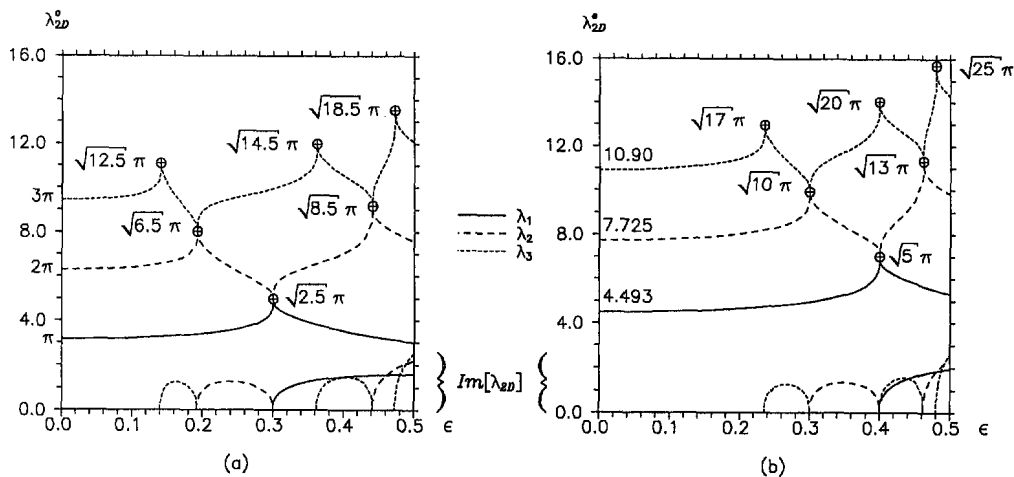


Fig. 5. Real and imaginary parts of first three (a) even and (b) odd two-dimensional eigenvalues, as a function of material properties through ϵ (eqn 64) ; For strongly orthotropic materials $\epsilon = 0$, for isotropic materials $\epsilon = 1/2$.

the error $(\bar{\lambda} - \lambda_{2D})/\lambda_{2D}$ is less than 5% if $\varepsilon < 0.12$ and $\varepsilon < 0.20$ for the first three odd and even eigenvalues, respectively. For the isotropic case ($\varepsilon = 0.5$), the error is 5.5% and 15.2%, respectively, and increases for higher eigenvalues.

The one-dimensional boundary solution obtained here gives the lower order ($\varepsilon \rightarrow 0$) two-dimensional *wide* boundary layer obtained by Horgan and Simmonds (1991) in their asymptotic analysis of a semi-infinite beam weak in shear performed in terms of the “slow” axial variable $\alpha = x/\sqrt{\rho}$. It is called wide boundary layer since it decays within a region that is wide compared to height. Correspondingly, the characteristic decay length $d = \ell(\ln 100)/\gamma_1$ (the distance over which all the stresses of the residual solution are below 1% of their values at $x = 0$) given by the one-dimensional model coincides with the asymptotic estimate derived from the elasticity solution for strongly orthotropic materials, i.e. for $\varepsilon \rightarrow 0$ (Choi and Horgan, 1977; Horgan, 1982). Making use of eqns (48), (52) and (53), the characteristic decay length is derived in the form $d = cH(E_1/G_{12})^{1/2}$, where $c = \ln 100/2\pi$ for even eigenfunctions (related to stretching) and $c = \ln 100/8.98682$ for odd eigenfunctions (i.e. for flexure problems).

Finally, it is worth noting that the present model cannot predict the *narrow* boundary layer obtained in Horgan and Simmonds (1991) in terms of the *fast* axial variable $\beta = \alpha/\varepsilon$; this circumstance suggests that the wide boundary layer is mainly associated to restrained axial warping and axial normal stress gradient, whereas the narrow boundary layer corresponds to the same effects in the transverse direction.

6. APPLICATIONS

Several comparisons with exact and numerical solutions for isotropic and orthotropic beams have been performed in order to check the accuracy of the proposed model. The analytical expressions of displacements and stresses for all the examples considered are reported in Appendix B.

6.1. Cantilever beams under flexure at infinity

The first example concerns isotropic and orthotropic cantilever beams of length $\ell \rightarrow \infty$ subject to a shear force \bar{F}_2' and an applied bending moment $\bar{F}_2'\ell$, such that the bending moment is zero at the clamped end section ($x = 0$). Due to the particular loading condition, only the self-equilibrated stress field due to the restrained warping is present at the clamped cross-section. Gregory and Gladwell (1982) solved the isotropic case by a projection method which avoids the overcompleteness problem when the eigenfunctions giving the proper stress singularities at the corners ($x = 0, y = \pm 1$) are added to the Papkovitch–Fadle set of eigenfunctions. Lin and Wan (1990) solved the orthotropic strip by recasting the governing equation in the form of a Fredholm integral equation of the first kind with a generalised Cauchy kernel. Figure 6 shows that the normal stresses at the clamped section given by the present one-dimensional model are in good agreement with the elasticity results, including the stress singularities. In fact, as briefly shown in Appendix B, the proposed model is able to predict the normal stress singularity of logarithmic form which is present at the corners, due to the transition between displacement and stress boundary conditions. Further details are given in Tullini and Savoia (1995).

6.2. Cantilever orthotropic beam subject to end shear force or uniform transverse load

A thick orthotropic beam with length-to-height ratio $\ell/H = 4$ and subject to a shear force \bar{F}_2' at the end section ($x_1 = \ell$) is considered first. The elastic properties of the beam, typical of a fibre-reinforced composite material, are $E_1 = 175$ GPa, $E_1/E_2 = 25$, $E_1/G_{12} = 50$, $\nu_{12} = 0.3$. Since no exact solutions can be found in the literature, the accuracy of the proposed model is assessed through comparison with results obtained via FEM. To this purpose, a 12×48 mesh of 8-node square isoparametric elements in plane stress is adopted (CPS8, ABAQUS 4/6), and stresses are computed at Gauss points of finite elements. The shear force \bar{F}_2' is applied through a St Venant parabolic shear traction distribution f_2 . Figures 7a,b show that normal and shear stress distributions given by the proposed one-dimensional model are in very close agreement with FEM results even in the

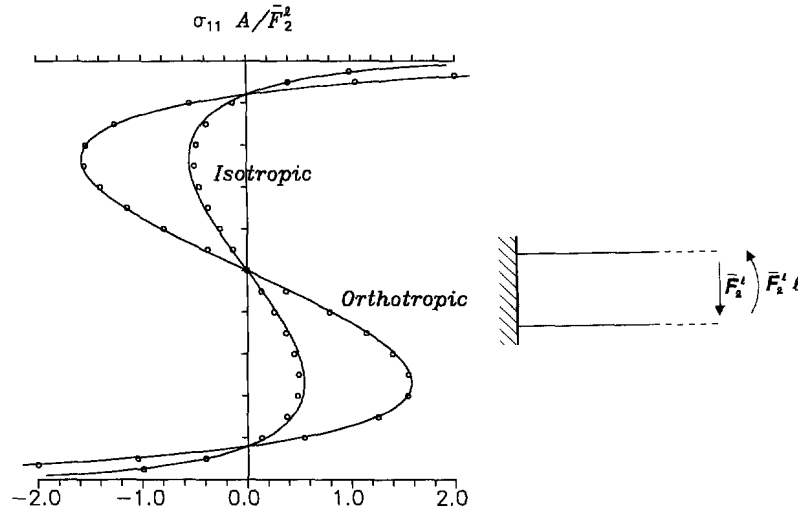


Fig. 6. Cantilever beam under flexure at infinity. Normal stress distribution at the clamped section ($x_1 = 0$) given by present one-dimensional model (—) is compared with two-dimensional solutions (○○○) by Gregory and Gladwell (1982) for the isotropic case ($\nu = 0$) and Lin and Wan (1990) for the orthotropic case ($E_1 = 12$ GPa, $E_2 = 6.44$ GPa, $G_{12} = 0.72$ GPa).

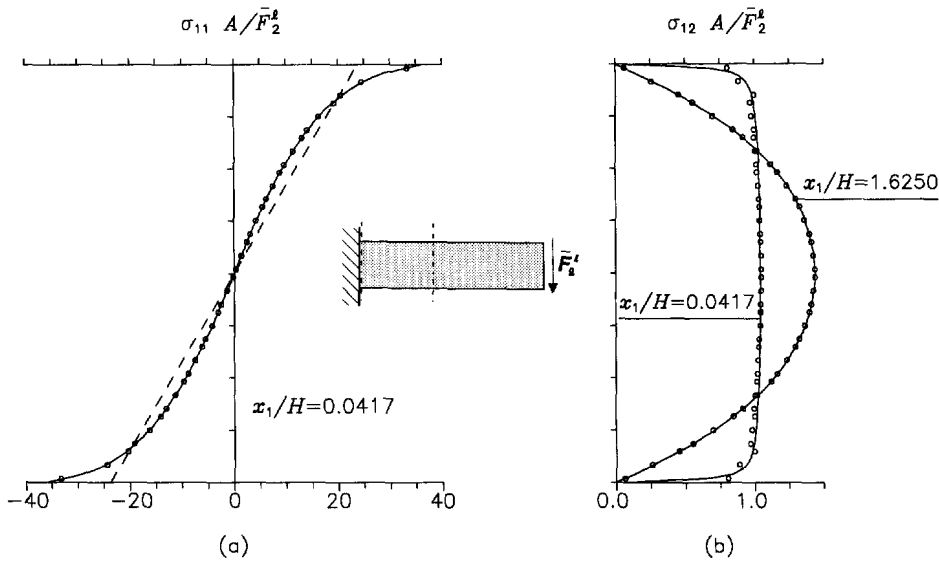


Fig. 7. Cantilever orthotropic beam ($\ell/H = 4$) subject to a shear force \bar{F}_2^0 at the end section: (a) normal and (b) shear stresses given by present analysis (—) are compared with FEM two-dimensional results (○○○) and Euler–Bernoulli solution (---).

neighbourhood of the clamped cross-section ($x_1/H = 0.0417$). Moreover, the presence of a stress boundary layer is clearly shown in Fig. 7b. In fact, the shear stress distribution is almost constant over the beam height near $x_1 = 0$, whereas it approaches the classical parabolic distribution far from the clamped section, where the solution is governed by the interior problem. In passing, it is to be remembered that the present model satisfies identically the stress-free condition at the top and bottom faces over the whole beam length.

For beams subject to an end shear force or a uniformly distributed transverse load ($q_{2b} = q_{2t} = q_0/2$), Figs 8a,b show the axial variation of normal stress σ_{11} at the beam top ($y = 1$), for different values of $E_1 H^2 / G_{12} \ell^2 (= 4\rho)$. The normal stress given by the Euler–Bernoulli solution is also reported. In both cases the normal stress singularities at the corner points ($x_1 = 0$) become stronger with the degree of orthotropy of the material [see also Tullini and Savoia (1995)]. In particular, eqns (B1c) and (B3c) reported in Appendix B show that the stress singularity depends on the square-root of ρ . Moreover, Fig. 8b shows that the beam under uniform load exhibits a typical “negative shear-lag” far from the

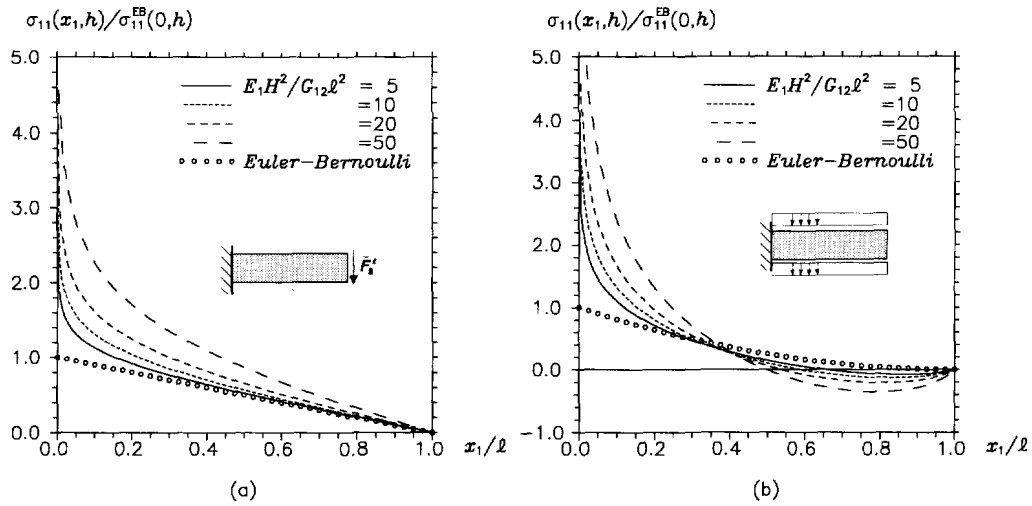


Fig. 8. Axial variation of the normal stress at the top face ($y = 1$) for a cantilever orthotropic beam subject to (a) a shear force at the end section and (b) a uniformly distributed transverse load, for different values of $4\rho = E_1 H^2 / G_{12} \ell^2$.

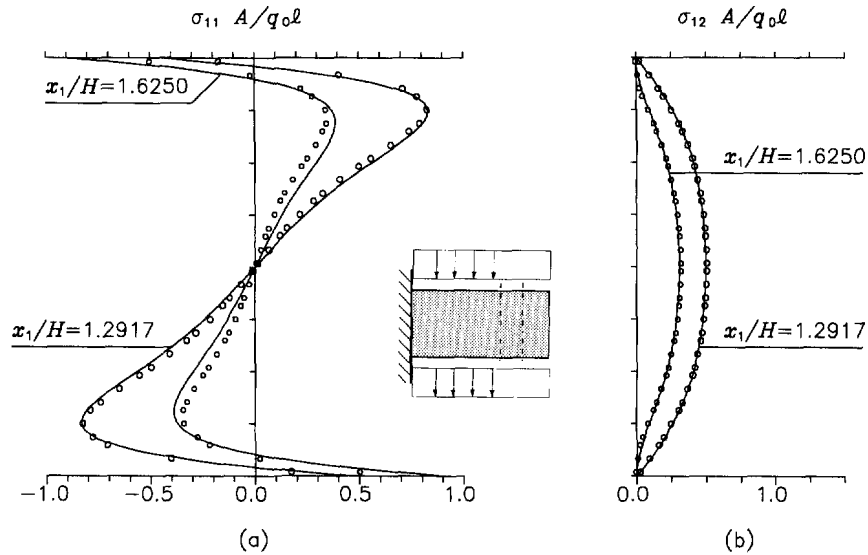


Fig. 9. Typical “shear-lag” phenomenon for a cantilever orthotropic beam ($\ell/H = 2$) under uniformly distributed transverse load: (a) normal and (b) shear stresses given by the present analysis (—) are compared with FEM two-dimensional results (○○○).

clamped end, resulting in additional self-equilibrated stresses due to warping variation. It is called “negative shear-lag” because it decreases the maximum values of normal stresses (at $y = \pm 1$), up to giving a stress reversal near the free end. For a thick ($\ell/H = 2$) orthotropic beam, resulting in $\rho = 12.5$, Figs 9a,b show that both normal and shear stresses given by the present model are in good agreement with FEM results, even where negative shear-lag phenomenon is dominant. Equation (B3c) reported in Appendix B shows that the normal stress contribution related to negative shear lag linearly depends on ρ . It is worth noting that the characteristic decay length of end effects for the material considered is $d = 3.62 H$, so that end effects arising from the clamped and the free extremities extend over the whole beam domain. Hence, refined engineering theories (Levinson, 1981; Rehfield and Murthy, 1982), where stresses and displacements are derived as functions of the stress resultants (bending moment, shear resultant) and their derivatives only, are typical interior solutions and cannot give accurate solutions.

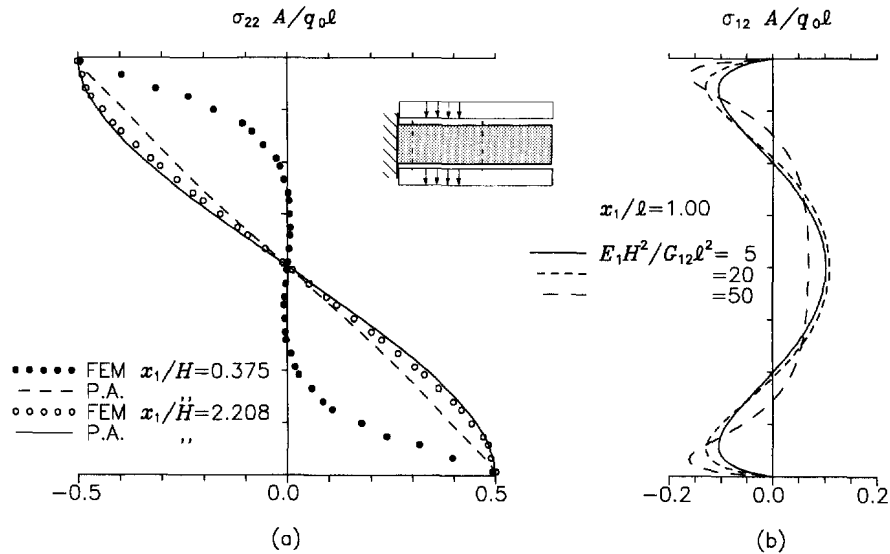


Fig. 10. Cantilever orthotropic beam ($\ell/H = 4$) under uniformly distributed transverse load: (a) transverse normal stress at $x_1/H = 0.375$ and 2.208 given by the present analysis and FEM two-dimensional solution; (b) non-vanishing shear stress at the beam free end, for different values of $4\rho = E_1 H^2 / G_{12} \ell^2$.

The main drawbacks of the assumption of transverse inextensibility are summarised in Figs 10a,b for a beam subject to uniformly distributed load. Figure 10a shows that the transverse normal stress σ_{22} , derived through integration of equilibrium equation in the transverse direction [see eqn (18)], are not accurate in the vicinity of the clamped cross-section. Moreover, Fig. 10b shows that the shear stress σ_{12} does not vanish at the free end ($x_1 = \ell$), where a (small) self-equilibrated distribution is still present. In fact, as is shown by eqn (7b), due to the constraint of cross-sectional inextensibility, only the shear resultant can be set equal to zero at the free end.

6.3. Simply-supported orthotropic beam under uniformly distributed transverse load

The last example refers to a simply-supported orthotropic beam ($\ell/H = 4$) subject to uniformly distributed load. The elastic properties are the same as in the previous example. The exact two-dimensional solution has been given by Pagano (1969) by representing the transverse load by means of a sine series expansion. In Figs 11a,b the normal stresses given by the present model and those obtained by retaining the principal part of the solution only are compared with the Pagano's solution. Figure 11a shows that the normal stress distributions near the end section ($x_1/\ell = 0.1$) and at the beam midspan ($x_1/\ell = 0.5$) given by the proposed one-dimensional model are in excellent agreement with the exact Pagano solution. On the contrary, if only the principal part of the solution is considered, the normal stresses are sufficiently accurate only at a considerable distance from the ends. Finally, Fig. 11a confirms that the classical Euler-Bernoulli hypothesis of cross-sections remaining plane after deformation (so ensuring linear normal stress distributions) is no longer reliable for strongly orthotropic materials.

The errors in the evaluation of the maximum value (at $x_1 = \ell/2, x_2 = h$) of normal stress with respect to the exact solution are reported in Fig. 11b as a function of the beam slenderness. Accurate normal stresses (with an error less than 2%) are given by the proposed model even for very thick beams ($\ell/H > 2.5$). Moreover, the same figure shows, as is to be expected, that the only principal part of the solution gives accurate results at the midspan for beams with $\ell/H > 4.5$. For instance, for the beam considered in Fig. 11a ($\ell/H = 4$), the errors of the present model with respect to the exact solution is 0.01%, whereas it rises up to 2.49% if only the principal part of the solution is considered. Finally, the Euler-Bernoulli solution is shown to be inaccurate even for slender beams, since it is not able to predict neither shear-lag phenomenon, nor end effects.

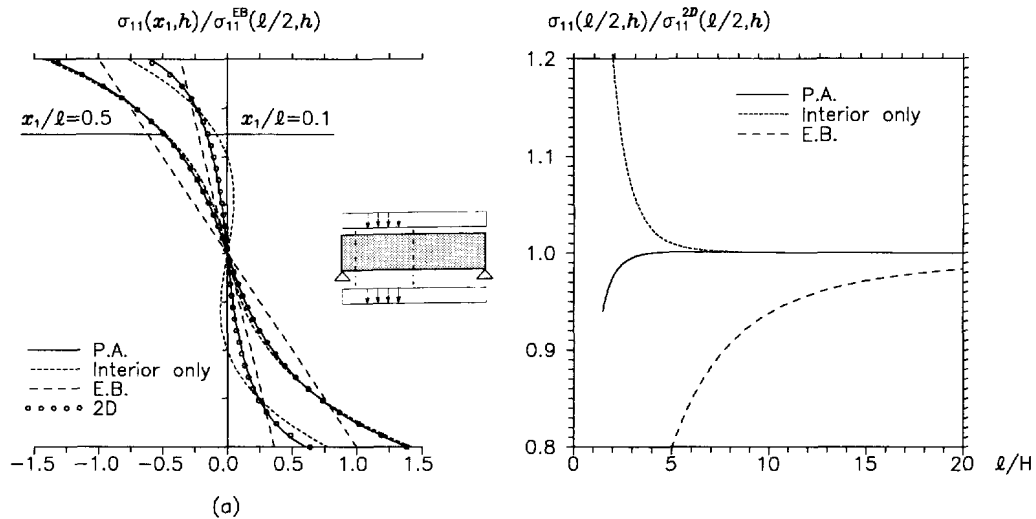


Fig. 11. Simply-supported orthotropic beam ($\ell/H = 4$) under uniformly distributed transverse load: (a) normal stress distributions near the end sections ($x_1/\ell = 0.1$) and at the beam midspan ($x_1/\ell = 0.5$); (b) error on maximum value of normal stress ($x_1 = \ell/2$, $x_2 = h$), for different values of length-to-height ratio. The two-dimensional solution is given in Pagano (1969).

7. FINAL REMARKS

The proposed one-dimensional theory is based on the kinematic assumption of inextensibility in the transverse direction (1) which is considered as an internal constraint; the corresponding equilibrium eqns (5)–(7) have been derived from the virtual work principle. In Sections 3 and 4 it has been proved that the proposed one-dimensional theory gives both interior and boundary two-dimensional elasticity solutions for strongly orthotropic materials, i.e. for ratio between shear modulus and axial Young modulus approaching zero. This result is in complete accordance with the theoretical predictions given by Sayir (1980). Performing an asymptotic expansion of elasticity equations, Sayir found that for orthotropic materials with $E_1/G_{12} = O(\ell^2/H^2)$ the classical hypothesis of cross-sections remaining plane after deformation is not admissible, and the governing equations reduce to eqns (2), (3) and (5)–(7) of the present model. His theoretical predictions were found to be in good agreement with experimental measurement of phase velocities of flexural waves even for short wavelengths (Sayir, 1987).

The effectiveness of beam models should be substantiated by checking their capability of describing both the principal and the residual part of the solution. For instance, the Levinson third-order theory (1981) gives the one-dimensional interior solution for a shear resultant linearly varying at most. For the same case, the Rehfield and Murthy (1982) engineering theory gives the exact two-dimensional solution (including transverse normal strain). These models are devoted to the principal part of the solution only, so that they may be inadequate for strongly orthotropic beams where end effects usually play a remarkable role.

Several models are based on axial displacement representation in terms of coordinate functions and unknown functions defined along the beam axis. Usually, the unknown functions are obtained by means of variational procedures by facing interior and boundary problems simultaneously, and the accuracy of the solution strongly depends on the set of coordinate functions adopted.

The potential of these models of describing the high stress gradients due to end effects can be verified by comparing the eigenvalues of the homogeneous associated problem with those obtained in Section 4. For instance, using as coordinate function a third-order polynomial (Hjelmstad, 1987; Laudiero and Savoia, 1990), the first eigenvalue λ_1^0 is equal to $\sqrt{140}/2$, with an error of 31.7% with respect to that given by eqn (53). The error can be drastically reduced by increasing the number of coordinate functions; for instance, using two and three (odd) Legendre polynomials (Savoia *et al.*, 1993a), the first eigenvalue equal

to 4.53571 and 4.49394 is obtained, respectively, with an error of 0.941% and 0.012% with respect to the exact value.

Acknowledgement—The financial support of the (Italian) National Council of Research (CNR-Contr. 93.02254.CT07) and of Human Capital Programme (Contr. No. CHRX-CT93-0383-DG 12 COMA) is gratefully acknowledged.

REFERENCES

- Antman, S. S. and Warner, W. H. (1966). Dynamical theory of hyperelastic rods. *Arch. Rat. Mech. Anal.* **23**, 135–162.
- Atligan, A. R. and Hodges, D. H. (1992). On the strain energy of laminated composite plates. *Int. J. Solids Structures* **29**, 2527–2543.
- Atligan, A. R., Hodges, D. H. and Fulton, M. V. (1991). Nonlinear deformation of composite beams: unification of cross-sectional and elastic analyses. *Appl. Mech. Rev.* **44**, S9–S15.
- Bauchau, O. A. (1985). A beam theory for anisotropic materials. *J. Appl. Mech. ASME* **52**, 416–422.
- Berdichevsky, V. L. (1981). On the energy of an elastic rod. *PMM* **45**, 518–529.
- Berdichevsky, V. L. and Kvashnina, S. S. (1976). On equations describing the transverse vibrations of elastic bars. *PMM* **40**, 120–135.
- Bickford, W. B. (1982). A consistent higher order beam theory. *Dev. Theor. Appl. Mech.* **11**, 137–150.
- Boley, B. A. and Tolins, I. S. (1956). On the stresses and deflections of rectangular beams. *J. Appl. Mech. ASME* **23**, 339–342.
- Borri, M. and Merlini, T. (1986). A large displacement formulation for anisotropic beam analysis. *Meccanica* **21**, 30–37.
- Cesnik, C. E. S. and Hodges, D. H. (1993). Variational-asymptotical analysis of initially curved and twisted composite beams. *Appl. Mech. Rev.* **46**, S211–S220.
- Choi, I. and Horgan, C. O. (1977). Saint-Venant's principle and end effects in anisotropic elasticity. *J. Appl. Mech. ASME* **44**, 424–430.
- Courant, R. and Hilbert, D. (1953). *Methods of Mathematical Physics*, Vol. I. Interscience, New York.
- Cowper, G. R. (1966). The shear coefficient in Timoshenko's beam theory. *J. Appl. Mech. ASME* **33**, 335–340.
- Crafter, E. C., Heise, R. M., Horgan, C. O. and Simmonds, J. G. (1993). The eigenvalues for a self-equilibrated, semi-infinite, anisotropic elastic strip. *J. Appl. Mech. ASME* **60**, 276–281.
- Donnell, L. H. (1952). Bending of rectangular beams. *J. Appl. Mech. ASME* **19**, 123.
- Donnell, L. H. (1976). *Beams, Plates and Shells*. McGraw Hill, New York.
- Duva, J. M. and Simmonds, J. G. (1990). Elementary, static beam theory is as accurate as you please. *J. Appl. Mech. ASME* **57**, 134–137.
- Duva, J. M. and Simmonds, J. G. (1991). The usefulness of elementary theory for the linear vibrations of layered, orthotropic elastic beams and corrections due to two-dimensional effects. *J. Appl. Mech. ASME* **58**, 175–180.
- Gatewood, B. E. and Dale, R. (1962). Note on two-dimensional stresses in long beams with spanwise variation of load and temperature. *J. Appl. Mech. ASME* **29**, 747–749.
- Giavotto, V., Borri, M., Mantegazza, P., Griringhelli, G., Carmaschi, V., Maffioli, G. C. and Mussi, F. (1983). Anisotropic beam theory and applications. *Comput. Structures* **16**, 403–413.
- Gregory, R. D. and Gladwell, I. (1982). The cantilever beams under tension, bending or flexure at infinity. *J. Elasticity* **12**, 317–343.
- Hashin, Z. (1967). Plane anisotropic beams. *J. Appl. Mech. ASME* **34**, 257–262.
- Heyliger, P. R. and Reddy, J. N. (1988). A higher order beam finite element for bending and vibration problems. *J. Sound Vibration* **126**, 309–326.
- Hildebrand, F. B. (1943). On the stress distribution in cantilever beams. *J. Math. Phys.* **22**, 188.
- Hjelmstad, K. D. (1987). Warping effects in transverse bending of thin-walled beams. *J. Eng. Mech. ASCE* **113**, 907–924.
- Horgan, C. O. (1982). Saint-Venant end effects in composites. *J. Compos. Mater.* **16**, 411–422.
- Horgan, C. O. and Simmonds, J. G. (1991). Asymptotic analysis of an end-loaded transversely isotropic, elastic, semi-infinite strip weak in shear. *Int. J. Solids Structures* **27**, 1895–1914.
- Kapania, R. K. and Raciti, S. (1989). Recent advances in analysis of laminated beams and plates, Part I: shear effects and buckling. *AIAA J.* **27**, 923–934.
- Koiter W. T. (1970). On the foundation of the linear theory of thin elastic shells. *Proc. Kon. Ned. Akad. Wet.* **B73**, 169–195.
- Ie, C. A. and Kosmatka, J. B. (1992). On the analysis of prismatic beams using first order warping functions. *Int. J. Solids Structures* **29**, 879–891.
- Ladevèze, P. (1983). Sur le principe de Saint-Venant en élasticité. *J. Mech. Theor. Appl.* **2**, 161–184.
- Laudiero, F. and Savoia, M. (1990). Shear strain effects in flexure and torsion of thin-walled beams with open or closed cross-sections. *Thin-Walled Structures* **10**, 87–119.
- Levinson, M. (1981). A new rectangular beam theory. *J. Sound Vibration* **74**, 81–87.
- Lewinski, T. (1987). On refined plate models based on kinematical assumptions. *Ing. Arch.* **57**, 133–146.
- Librescu, L. (1975). *Elastostatics and Kinetics of Anisotropic and Heterogeneous Shell-Type Structures*. Nordhoff I. P., Leyden.
- Lin, Y. H. and Wan, F. Y. M. (1990). Bending and flexure of semi-infinite cantilevered orthotropic strips. *Comput. Structures* **35**, 349–359.
- Massonet, C. E. (1983). A new approach (including shear lag) to elementary mechanics of materials. *Int. J. Solids Structures* **19**, 33–54.
- Mathúna, D. (1989). *Mechanics, Boundary Layers, and Function Spaces*. Birkhäuser, Boston.
- Naghdi, P. M. (1972). The theory of shells and plates. In *Handbuch der Physik* (Edited by S. Flugge), Vol VI-2. pp. 425–640. Springer-Verlag, Berlin.

- Nair, S. and Reissner, E. (1975). Improved upper and lower bounds for deflections of orthotropic cantilever beams. *Int. J. Solids Structures* **11**, 961–971.
- Pagano, N. J. (1969). Exact solutions for composite laminates in cylindrical bending. *J. Compos. Mater.* **3**, 398–411.
- Podio Guidugli, P. (1989). An exact derivation of the thin plate equation. *J. Elasticity* **22**, 121–133.
- Reddy, J. N. (1987). A generalization of two-dimensional theories of laminated composite plates. *Commun. Appl. Numer. Meth.* **3**, 173–180.
- Reddy, J. N. and Robbins, D. H. (1994). Theories and computational models for composite laminates. *Appl. Mech. Rev.* **47**, 147–169.
- Rehfield, L. W. and Murthy, P. L. N. (1982). Toward a new engineering theory of bending: fundamentals. *AIAA J.* **20**, 693–699.
- Reissner, E. (1946). Analysis of shear lag in box beams by the principle of the minimum of potential energy. *Quart. Appl. Math.* **4**, 268–278.
- Renton, J. D. (1991). Generalized beam theory applied to shear stiffness. *Int. J. Solids Structures* **27**, 1955–1967.
- Rychter, Z. (1988). A simple and accurate beam theory. *Acta Mech.* **75**, 57–62.
- Savoia, M. (1996). On the accuracy of one-dimensional models for multilayered composite beams. *Int. J. Solids Structures* **33**, 521–544.
- Savoia, M., Laudiero, F. and Tralli, A. (1993a). A refined theory for laminated beams: Part I—A new high order approach. *Meccanica* **28**, 39–51.
- Savoia, M., Tralli, A. and Laudiero, F. (1993b). A refined theory for laminated beams: Part II—An iterative variational approach. *Meccanica* **28**, 217–225.
- Savoia, M., Laudiero, F. and Tralli, A. (1994). A two-dimensional theory for the analysis of laminated plates. *Comput. Mech.* **14**, 38–51.
- Sayir, M. (1980). Flexural vibrations of strongly anisotropic beams. *Ing. Arch.* **49**, 309–330.
- Sayir, M. (1987). Theoretical and experimental results on the dynamic behaviour of composite beams, plates and shells. In *Refined Dynamical Theories of Beams, Plates and Shells* (Edited by C. A. Brebbia and S. A. Orszag) Lectures Notes in Engineering, **28**, pp. 72–88. Springer-Verlag, Berlin.
- Soler, A. I. (1968). Higher order effects in thick, rectangular elastic beams. *Int. J. Solids Structures* **4**, 723–739.
- Timoshenko, S. P. and Goodier, J. N. (1970). *Theory of Elasticity*, 3rd edn. McGraw Hill, New York.
- Truesdell, C. and Noll, W. (1965). The non linear field theories of mechanics. In *Encyclopedia of Physics* (Edited by S. Flugge), III/3. Springer-Verlag, Berlin.
- Tsai, H. and Soler, A. I. (1970). Approximate theory for locally loaded plane orthotropic beams. *Int. J. Solids Structures* **6**, 1055–1068.
- Tullini, N. and Savoia, M. (1995). Logarithmic stress singularities at clamped-free corners of a cantilever orthotropic beam under flexure. *Compos. Structures* **32**, 659–666.
- Wang, M. Z., Ting, T. C. T. and Yan G. (1993). The anisotropic elastic semi-infinite strip. *Quart. Appl. Math.* **51**, 283–297.

APPENDIX A

Completeness of eigenfunction expansion

Eqns (22b,d) can be rewritten in the form of Fredholm equation of second kind as:

$$P_n = \rho \mathbf{T}(P_{n-2}) \quad \text{where} \quad \mathbf{T}(P_{n-2}) = \int_0^1 K(y, t) P_{n-2}(t) dt \quad (\text{A1})$$

and $K(y, t)$ is the kernel of linear integral operator \mathbf{T} . Making use of eqns (21), $K(y, t)$ can be written as:

$$K^e(y, t) = \begin{cases} (t^2 + y^2)/2 - y, & y \leq t \\ (t^2 + y^2)/2 - t, & t \leq y \end{cases}$$

$$K^o(y, t) = \begin{cases} yt(t^2 + y^2)/2 + t, & y \leq t \\ yt(t^2 + y^2)/2 + y, & t \leq y \end{cases} \quad (\text{A2})$$

respectively, for even and odd polynomials. Both kernels are symmetric, i.e. $K(y, t) = K(t, y)$.

It is easy to verify that the eigenvalue problem (47) with boundary conditions (51) reduces to the homogeneous integral equation:

$$U_n = \lambda_n^2 \mathbf{T}(U_n). \quad (\text{A3})$$

Therefore, the symmetry of the kernels (A2) assures the validity of completeness and expansion theorems for the eigenvalue problem (47) [see Courant and Hilbert (1953), Chapters III and IV, Section 14].

Derivation of eqns (54)

Eqn (A1a) is applied recursively, so obtaining

$$P_{2n+2} = \rho^n \mathbf{T}^n(P_2), \quad P_{2n+3} = \rho^n \mathbf{T}^n(P_3) \quad (\text{A4})$$

where the kernel of \mathbf{T}^n is:

$$K_n = \int_0^1 K_{n-1}(y, s)K(s, t) ds \tag{A5}$$

and $K_1 = K$. Since K is symmetric, the iterated kernel (A5) can be expanded by means of the set of eigenfunctions (49) as:

$$K_n(y, t) = \sum_{j=1}^{\infty} \frac{1}{\lambda_j^{2n}} \frac{U_j(y)U_j(t)}{\|U_j\|_{L_2}^2} \quad \text{for } n \geq 1 \tag{A6}$$

where $\|\cdot\|_{L_2}$ is the $L_2([0, 1])$ -norm. The series (A6) converges absolutely and uniformly also for $n = 1$; in fact, $K_1 = K$ is positive-definite and the Mercer theorem holds [Courant and Hilbert (1953), p. 138]. Hence, making use of eqns (A4) and (A6) the polynomials used to solve the interior problem can be expanded as:

$$\{P_{2n+2}, P_{2n+3}\} = \rho^n \sum_{j=1}^{\infty} \frac{U_j(y)}{\lambda_j^{2n}} \frac{\int_0^1 U_j(t)\{P_2(t), P_3(t)\} dt}{\int_0^1 U_j^2(t) dt} \tag{A7}$$

and straightforward computation yields eqns (54).

Sufficient condition for convergence of interior solution

Eqns (54) can be rewritten as follows:

$$P_{2n} = -2 \left(\frac{\rho}{\lambda_1^e}\right)^n \sum_{j=1}^{\infty} (-1)^j \left(\frac{\lambda_1^e}{\lambda_j^e}\right)^{2n} \cos \lambda_j^e y$$

$$P_{2n+1} = -\frac{2}{3} \left(\frac{\rho}{\lambda_1^o}\right)^n \sum_{j=1}^{\infty} \left(\frac{\lambda_1^o}{\lambda_j^o}\right)^{2n} \frac{\sin \lambda_j^o y}{\sin \lambda_j^o} \tag{A8}$$

The series appearing in eqns (A8) are convergent, so that an upper bound for eqns (54) can be found as follows:

$$\{|P_{2n}|, |P_{2n+1}|\} \leq C \left\{ \left(\frac{\rho}{\lambda_1^e}\right)^n, \left(\frac{\rho}{\lambda_1^o}\right)^n \right\} \tag{A9}$$

Finally, with reference to eqns (37) and (44), if $q_1^{(2n)}$ and $T^{(2n)}$ are bounded, sufficient conditions for the convergence of the interior problem are $\rho/\lambda_1^e \leq 1$ and $\rho/\lambda_1^o \leq 1$ (i.e. $\rho < 9.87$ and $\rho < 20.19$) for stretching and flexure problem, respectively. The same procedure is used to obtain the sufficient condition for convergence of the shear factor \bar{k} reported in eqn (43).

APPENDIX B

Displacement and stress fields given by the present one-dimensional model for the cases considered in the numerical applications are reported hereafter.

Orthotropic beam clamped at $x = 0$ and subject to a constant shear resultant $Q(x) = \bar{F}_2^1$

$$u_1 = -\frac{\bar{F}_2^1 \ell^2}{2E_1 I} h \left[x(2-x)y + \frac{\rho}{15}(5y^3 - 3y) - \frac{4\rho}{3} \sum_{n=1}^{\infty} \frac{1}{\lambda_n^{o^2}} \varphi_n(x) U_n^o(y) \right]$$

$$u_2 = \frac{\bar{F}_2^1 \ell^3}{3E_1 I} \left\{ \frac{x^2}{2}(3-x) + \frac{6\rho}{5}x - 2\rho\sqrt{\rho} \sum_{n=1}^{\infty} \frac{1}{\lambda_n^{o^3}} [\tanh \gamma_n^o + \bar{\varphi}_n(x)] \right\}$$

$$\sigma_{11} = -\frac{\bar{F}_2^1 \ell}{A} \frac{1}{h} \left[3(1-x)y - \sqrt{\rho} \sum_{n=1}^{\infty} \frac{2}{\lambda_n^o} \bar{\varphi}_n(x) U_n^o(y) \right]$$

$$\sigma_{12} = \frac{\bar{F}_2^1}{A} \left[\frac{3}{2}(1-y^2) + \sum_{n=1}^{\infty} \frac{2}{\lambda_n^o} \varphi_n(x) \frac{\cos \lambda_n^o y - \cos \lambda_n^o}{\sin \lambda_n^o} \right]$$

$$\sigma_{22} = \frac{\bar{F}_2^1}{A} \frac{h}{\ell \sqrt{\rho}} \sum_{n=1}^{\infty} \frac{2}{\lambda_n^o} \bar{\varphi}_n(x) [y - U_n^o(y)] \tag{B1}$$

where:

$$\bar{\varphi}_n(x) = \sinh \gamma_n x - \tanh \gamma_n \cosh \gamma_n x. \quad (\text{B2})$$

The stress components in eqns (B1c,d) and the lateral deflection (B1b) have been derived in Hildebrand (1943) and Nair and Reissner (1975), respectively, making use of the Airy stress function. In these papers, the internal constraint of transverse inextensibility has been implicitly introduced by assuming $E_2 = \infty$.

It is worth noting that the normal stress σ_{11} presents stress singularities at the clamped end section ($x = 0, y = \pm 1$), due to the transition between the stress-free ($\sigma_{12} = 0$) boundary condition at $y = \pm 1$ and the null displacement ($u_1 = u_2 = 0$) boundary condition at $x = 0$; in fact, for n sufficiently large, eqn (53) gives $\lambda_n^o \approx (2n+1)\pi/2$ and $\tanh \gamma_n \approx 1$, so that the series in eqn (B1c) (representing the residual part of the solution), when evaluated at the corner points reduces to the (divergent) armonic series $-1/(2n+1)\pi$ [see Tullini and Savoia (1995) for details]. Moreover, the shear stress is discontinuous between ($x = 0, y = \pm 1$) and ($x = 0^+, y = \pm 1$). In fact, first of all, it can be verified that the series in eqn (B1d), when evaluated at $x = 0$ converges to $(3y^2 - 1)/2$ and, correspondingly, σ_{12} takes the constant value F_2^o/A over the whole clamped cross-section. Moreover, the principal part of the solution as well as the individual contributions of the eigenfunctions, satisfy the stress-free condition at the lateral surfaces.

Cantilever beam clamped at $x = 0$ and subject to uniform transverse load $q_2(x) = q_0$

$$\begin{aligned} u_1 &= -\frac{q_0 \ell^3}{6E_1 I} h \left[x(3 - 3x + x^2)y + \frac{\rho}{5}(1-x)(5y^3 - 3y) - 4\rho \sum_{n=1}^{\infty} \frac{1}{\lambda_n^o} \left(\varphi_n - \frac{\sinh \gamma_n^o x}{\gamma_n^o \cosh \gamma_n^o} \right) U_n^o \right] \\ u_2 &= \frac{q_0 \ell^4}{8E_1 I} \left[\frac{x^2}{3}(6 - 4x + x^2) + \frac{8\rho}{5}x(2-x) - \frac{16}{3}\rho\sqrt{\rho} \sum_{n=1}^{\infty} \frac{1}{\lambda_n^o} \left(\tanh \gamma_n^o + \bar{\varphi}_n - \frac{\cosh \gamma_n^o x - 1}{\gamma_n^o \cosh \gamma_n^o} \right) \right] \\ \sigma_{11} &= -\frac{q_0 \ell}{A} \frac{\ell}{h} \left[\frac{3}{2}(1-x)^2 y - \frac{\rho}{10}(5y^3 - 3y) - 2\sqrt{\rho} \sum_{n=1}^{\infty} \frac{2}{\lambda_n^o} \left(\bar{\varphi}_n - \frac{\cosh \gamma_n^o x}{\gamma_n^o \cosh \gamma_n^o} \right) U_n^o \right] \\ \sigma_{12} &= \frac{q_0 \ell}{A} \left[\frac{3}{2}(1-x)(1-y^2) + \sum_{n=1}^{\infty} \frac{2}{\lambda_n^o} \left(\varphi_n - \frac{\sinh \gamma_n^o x}{\gamma_n^o \cosh \gamma_n^o} \right) \frac{\cos \lambda_n^o y - \cos \lambda_n^o}{\sin \lambda_n^o} \right] \\ \sigma_{22} &= \frac{q_0}{2} \left[\frac{1}{2}(3y - y^3) + \frac{2}{\sqrt{\rho}} \sum_{n=1}^{\infty} \frac{1}{\lambda_n^o} \left(\bar{\varphi}_n - \frac{\cosh \gamma_n^o x}{\gamma_n^o \cosh \gamma_n^o} \right) (y - U_n^o) \right]. \end{aligned} \quad (\text{B3})$$

Simple supported beam under uniform transverse load $q_2(x) = q_0$

$$\begin{aligned} u_1 &= -\frac{q_0 \ell^3 h}{24E_1 I} \left[(1 - 6x^2 + 4x^3)y + \frac{2\rho}{5}(1-2x)(5y^3 - 3y) + 16\rho\sqrt{\rho} \sum_{n=1}^{\infty} \frac{\sinh \gamma_n^o (1-2x)/2}{\lambda_n^o \cosh \gamma_n^o/2} U_n^o \right] \\ u_2 &= \frac{q_0 \ell^4}{24E_1 I} \left[x(1 - 2x^2 + x^3) + \frac{24\rho}{5}x(1-x) + 16\rho^2 \sum_{n=1}^{\infty} \frac{\sinh \gamma_n^o (1-2x)/2 - \cosh \gamma_n^o/2}{\lambda_n^o \cosh \gamma_n^o/2} \right] \\ \sigma_{11} &= \frac{q_0 \ell^2}{8I} h \left[4x(1-x)y + \frac{4\rho}{15}(5y^3 - 3y) - \frac{16\rho}{3} \sum_{n=1}^{\infty} \frac{\cosh \gamma_n^o (1-2x)/2}{\lambda_n^o \cosh \gamma_n^o/2} U_n^o \right] \\ \sigma_{12} &= \frac{q_0 \ell}{2A} \left[\frac{3}{2}(1-2x)(1-y^2) + 4\sqrt{\rho} \sum_{n=1}^{\infty} \frac{\sinh \gamma_n^o (1-2x)/2}{\lambda_n^o \cosh \gamma_n^o/2} \frac{\cos \lambda_n^o y - \cos \lambda_n^o}{\sin \lambda_n^o} \right] \\ \sigma_{22} &= \frac{q_0}{2} \left[\frac{1}{2}(3y - y^3) + 2 \sum_{n=1}^{\infty} \frac{\cosh \gamma_n^o (1-2x)/2}{\lambda_n^o \cosh \gamma_n^o/2} (y - U_n^o) \right]. \end{aligned} \quad (\text{B4})$$